Photophysical properties of some novel tetraphenylimidazole derived BODIPY based fluorescent molecular rotors

Bhupendra Kumar Dwivedi, Vishwa Deepak Singh, Yogesh Kumar and Daya Shankar Pandey*

Department of Chemistry, Institute of Science, Banaras Hindu University, Varanasi–221 005 (UP), India

Contents

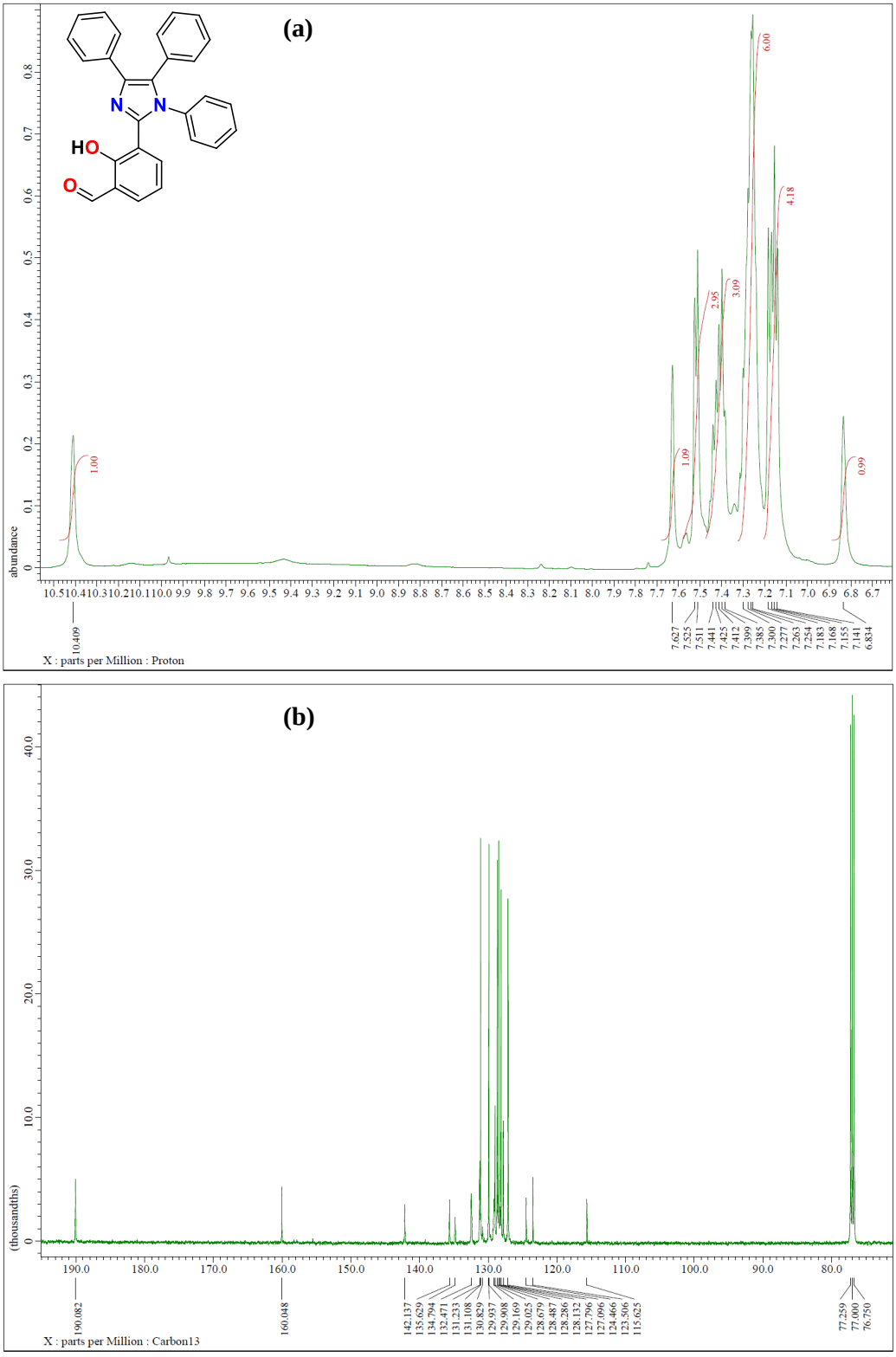

Fig. S1 ^{1}H (a) and **^{13}C** (b) NMR spectra of **4a** in $CDCl_3$.

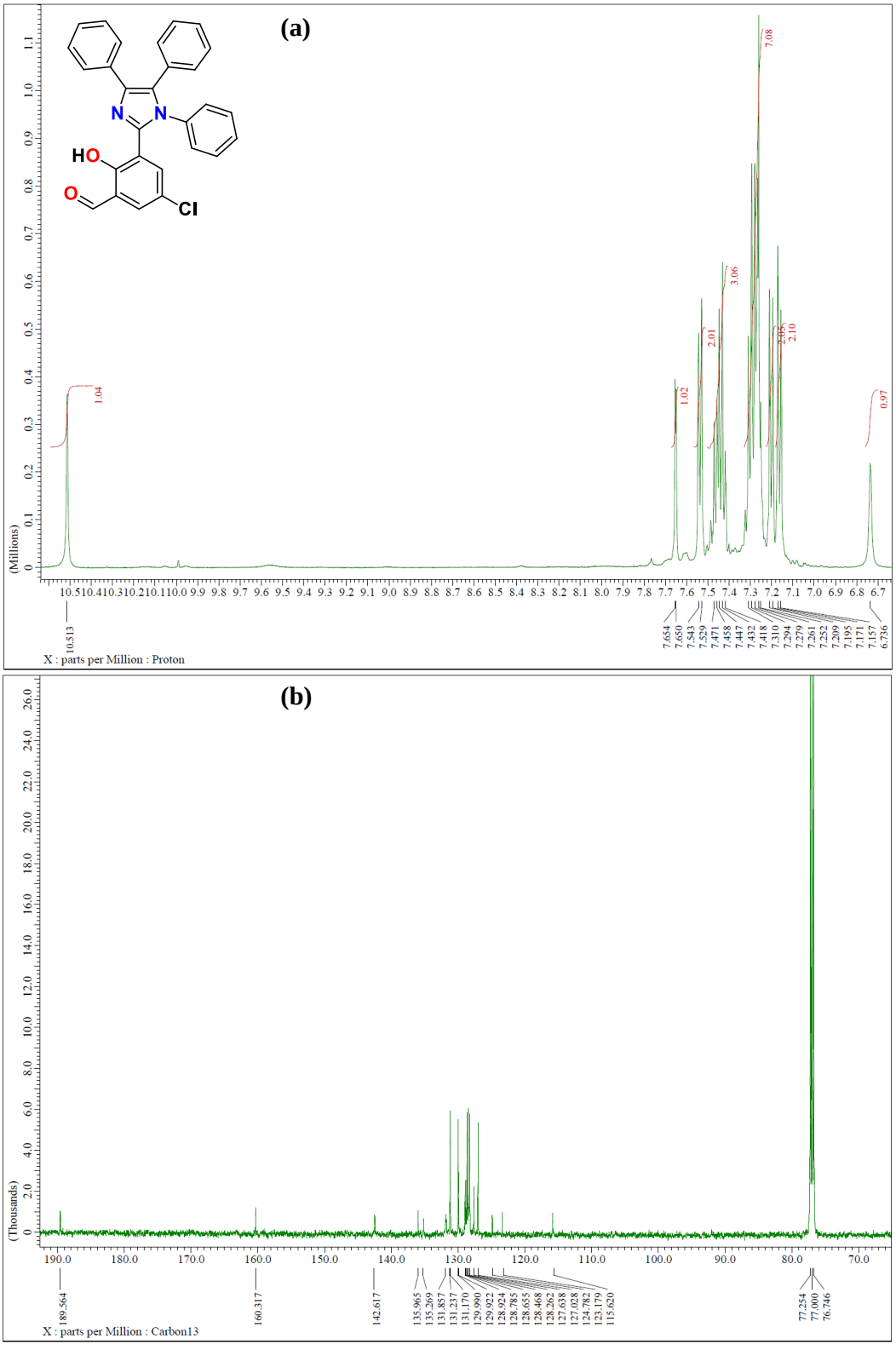

Fig. S2 ^{1}H (a) and **^{13}C** (b) NMR spectra of **4b** in $CDCl_3$.

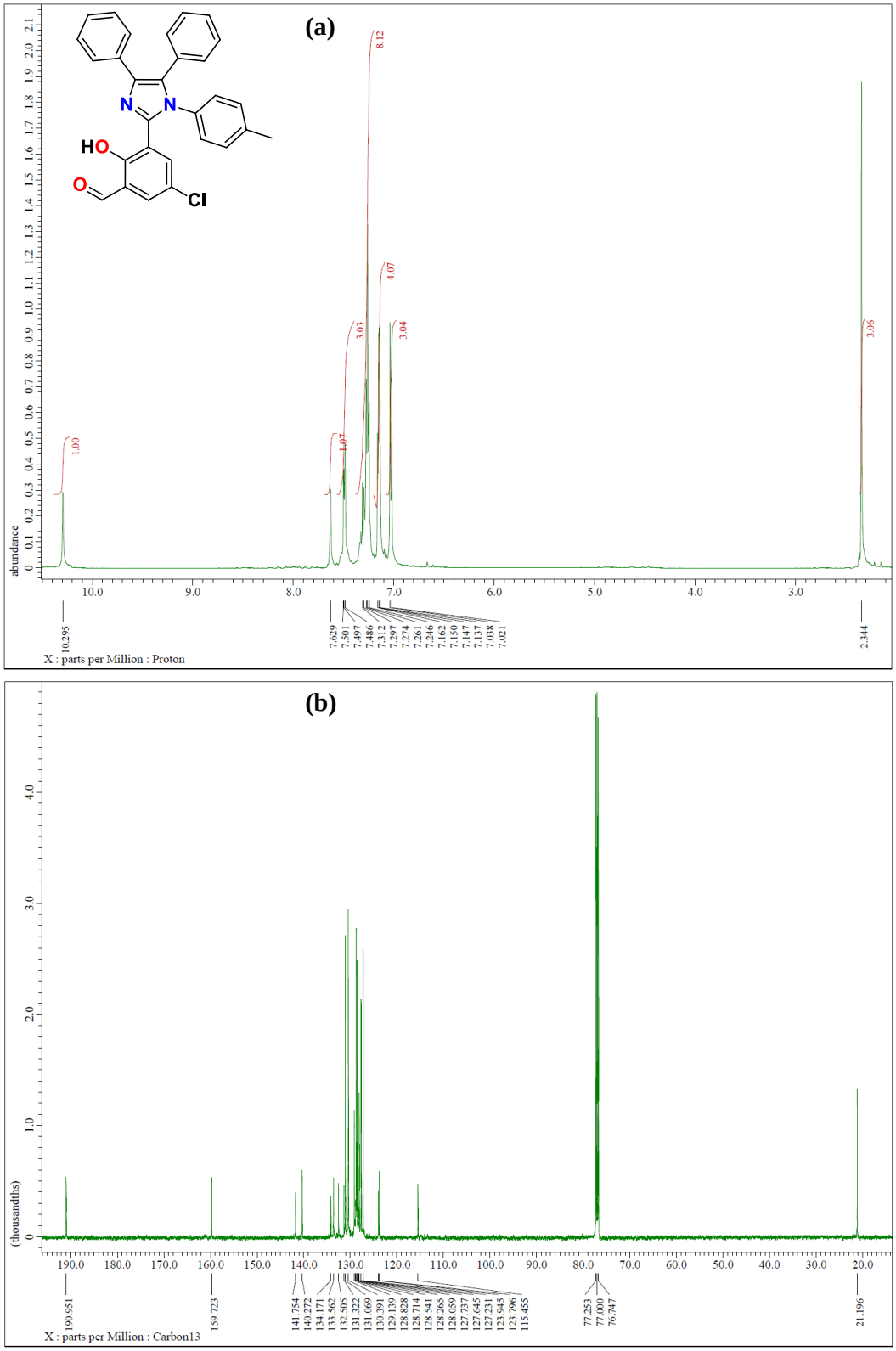

Fig. S3 ^{1}H (a) and **^{13}C** (b) NMR spectra of **4c** in $CDCl_3$.

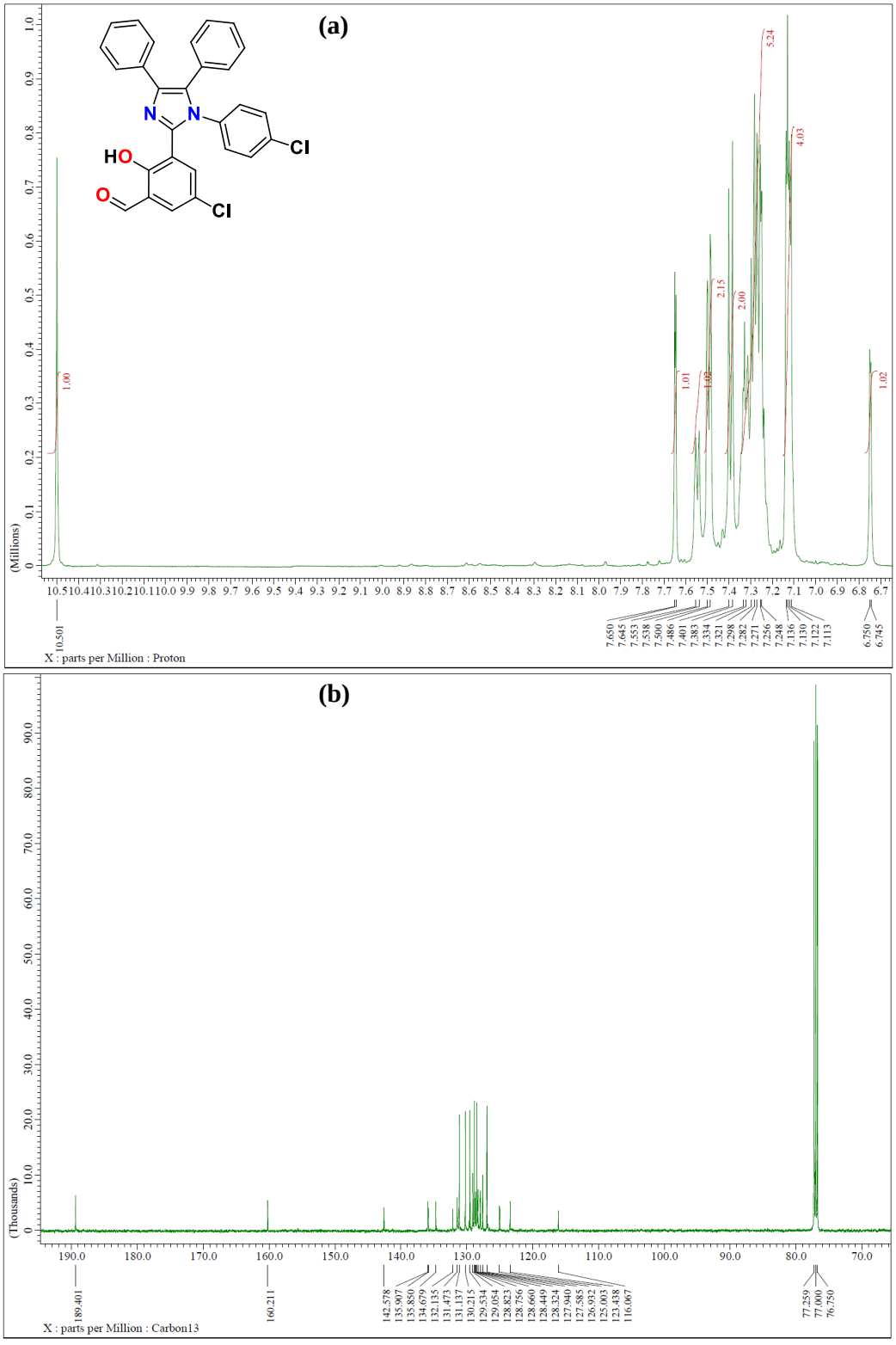

Fig. S4 ^{1}H (a) and **^{13}C** (b) NMR spectra of **4d** in $CDCl_3$.

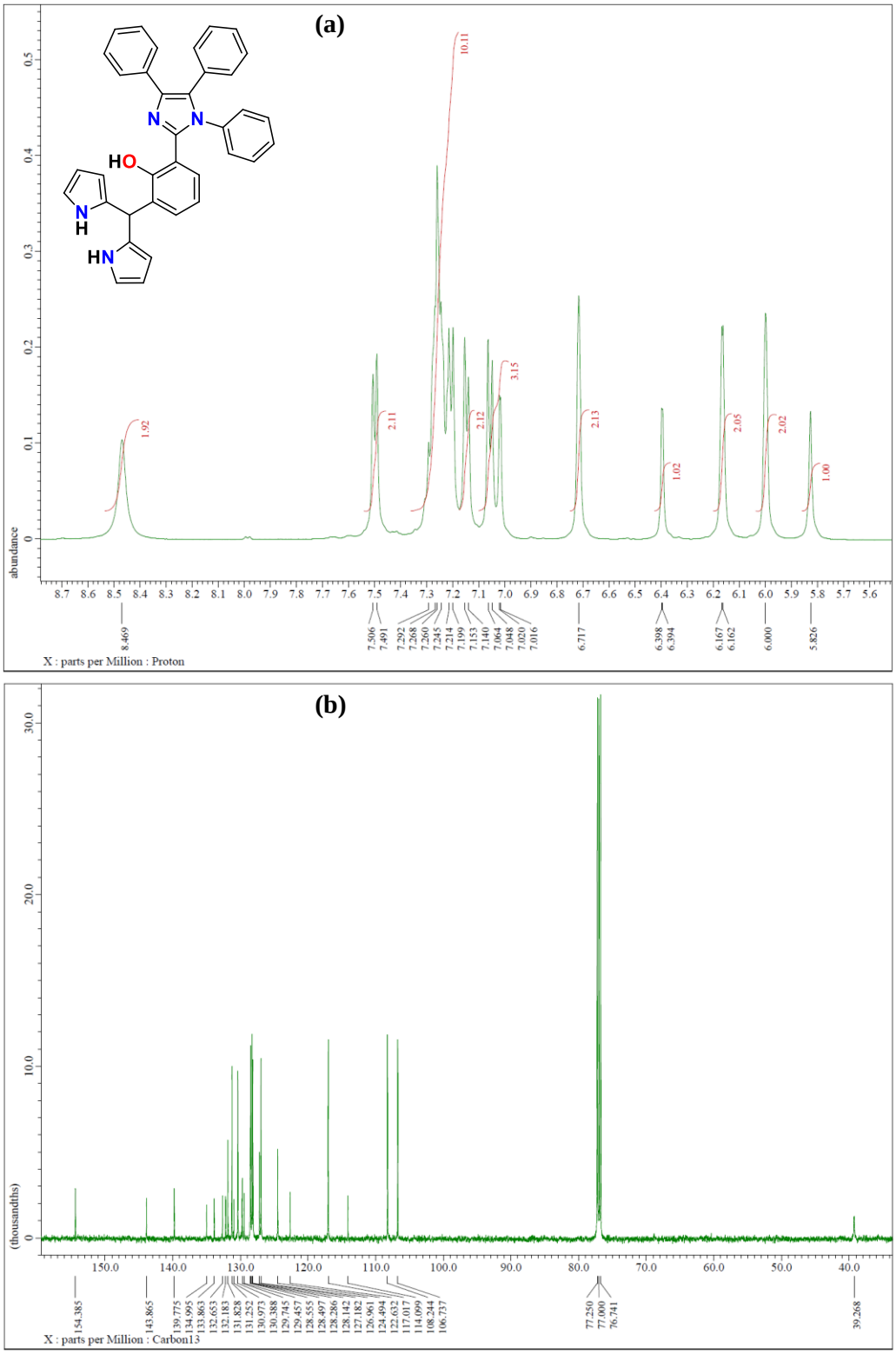

Fig. S5 ^{1}H (a) and **^{13}C** (b) NMR spectra of **5a** in $CDCl_3$.

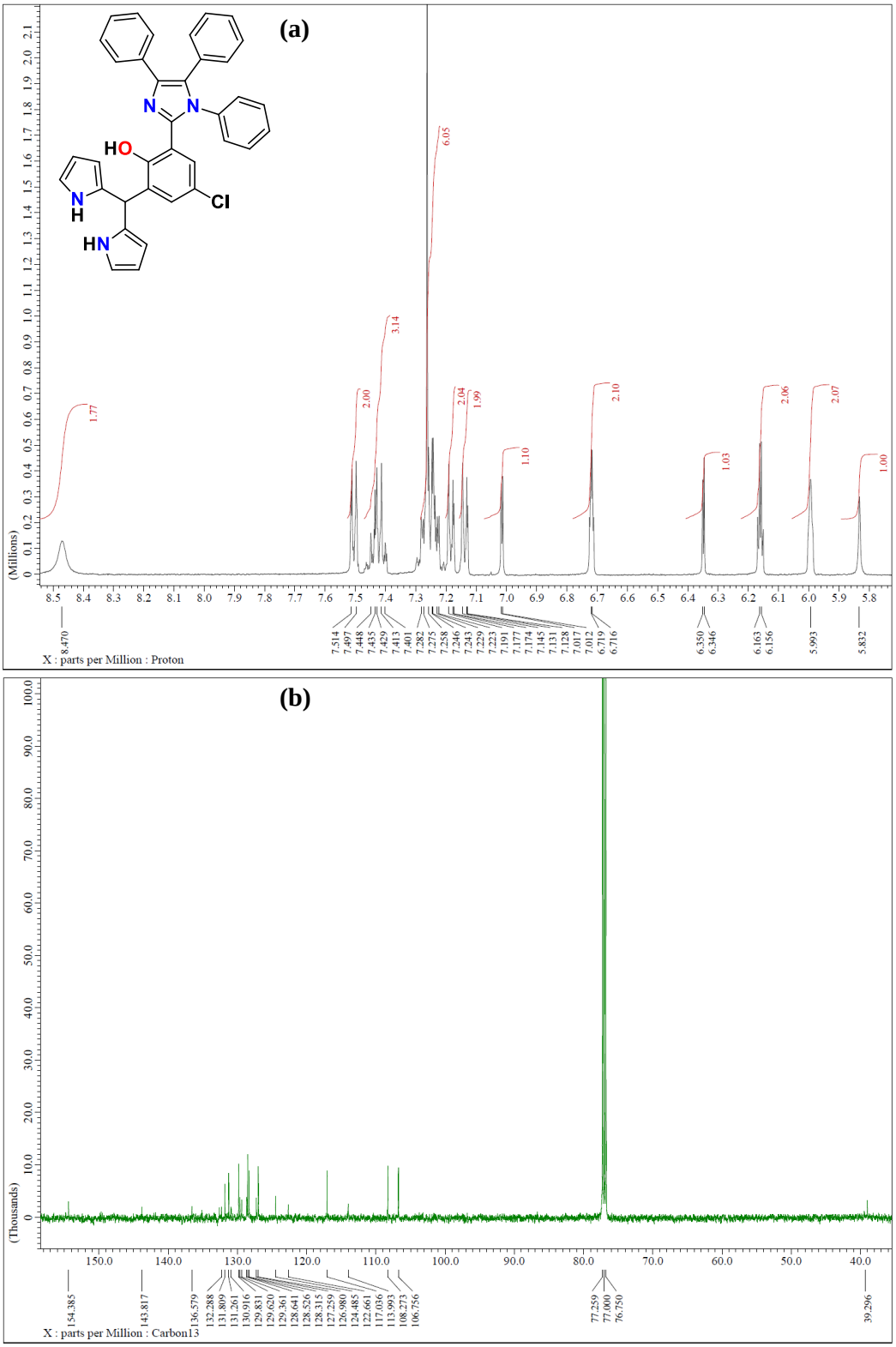

Fig. S6 ^{1}H (a) and **^{13}C** (b) NMR spectra of **5b** in $CDCl_3$.

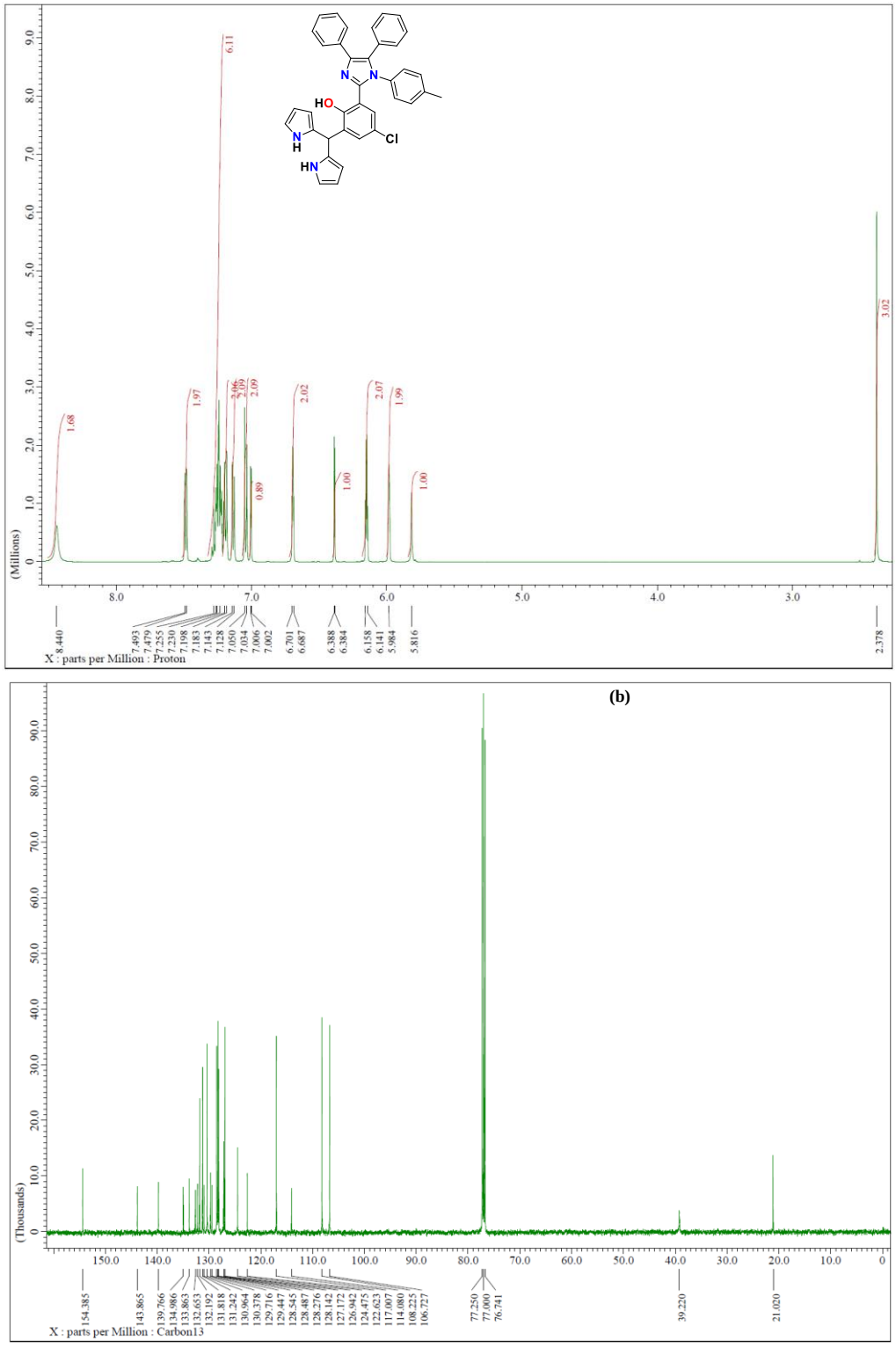

Fig. S7 ^{1}**H** (a) and ^{13}**C** (b) NMR spectra of **5c** in $CDCl_3$

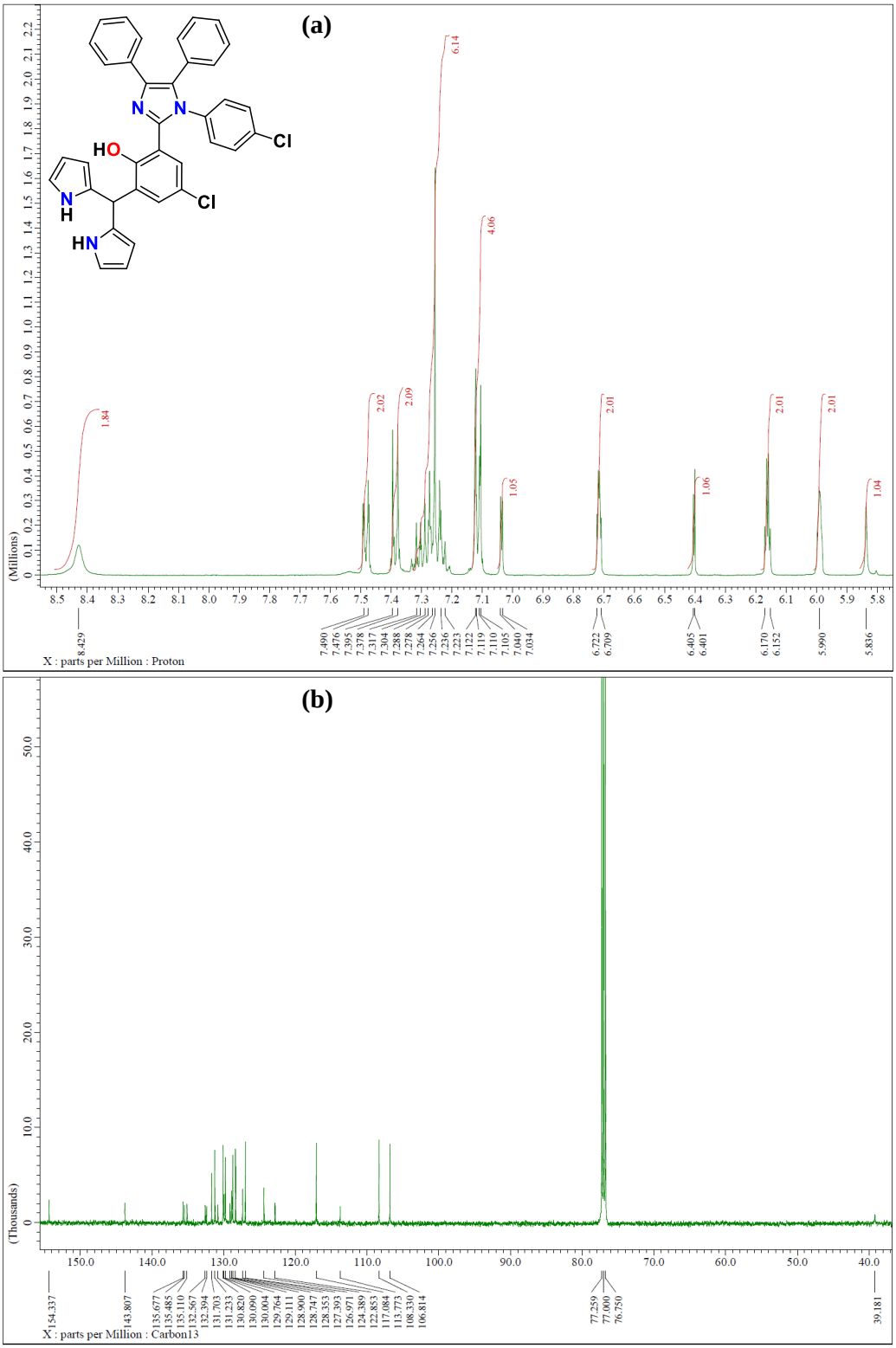

Fig. S8 **^{1}H** (a) and **^{13}C** (b) NMR spectra of **5d** in $CDCl_3$.

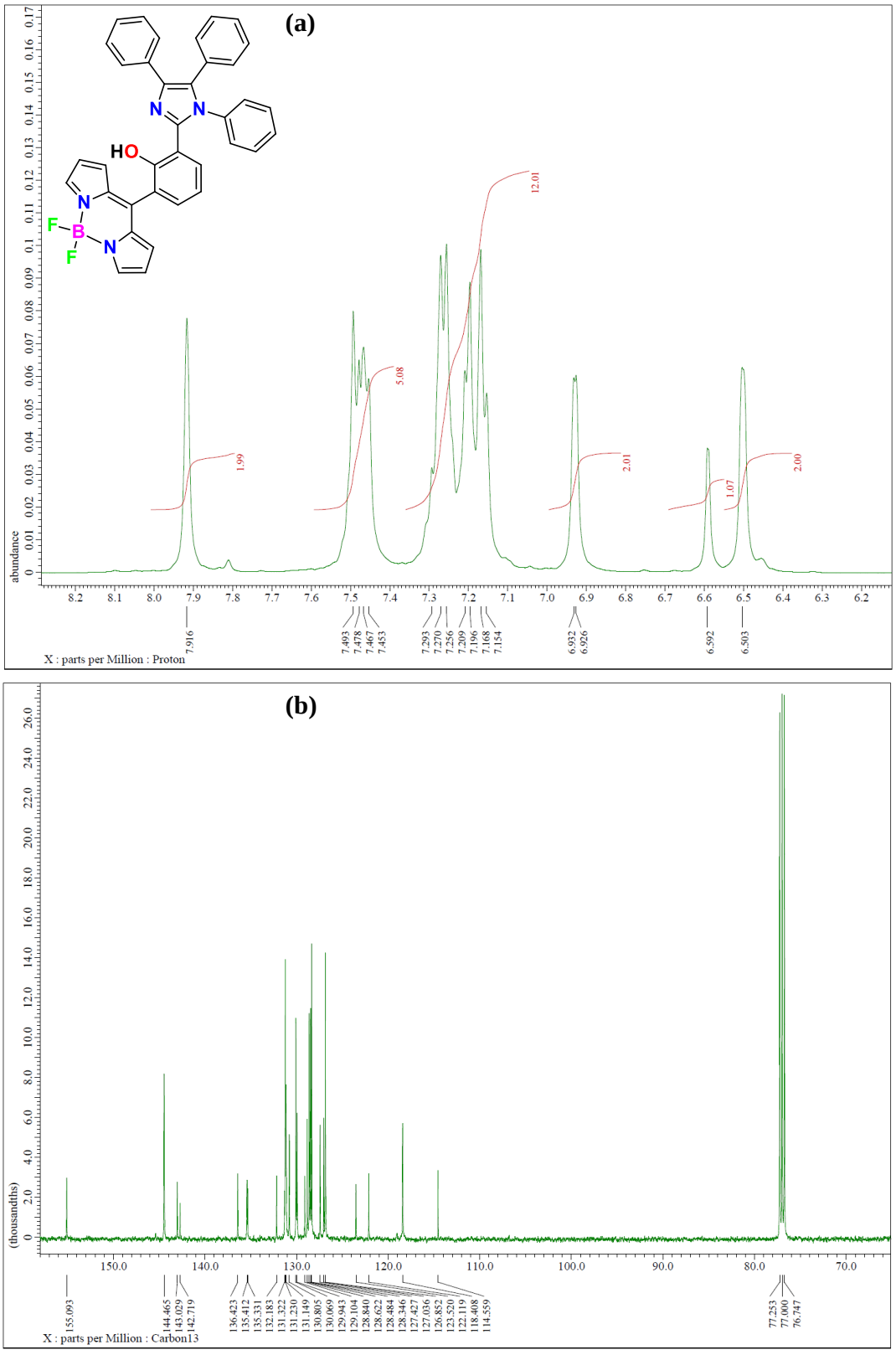

Fig. S9 **^{1}H** (a) and **^{13}C** (b) NMR spectra of **HPIB1** in $CDCl_3$

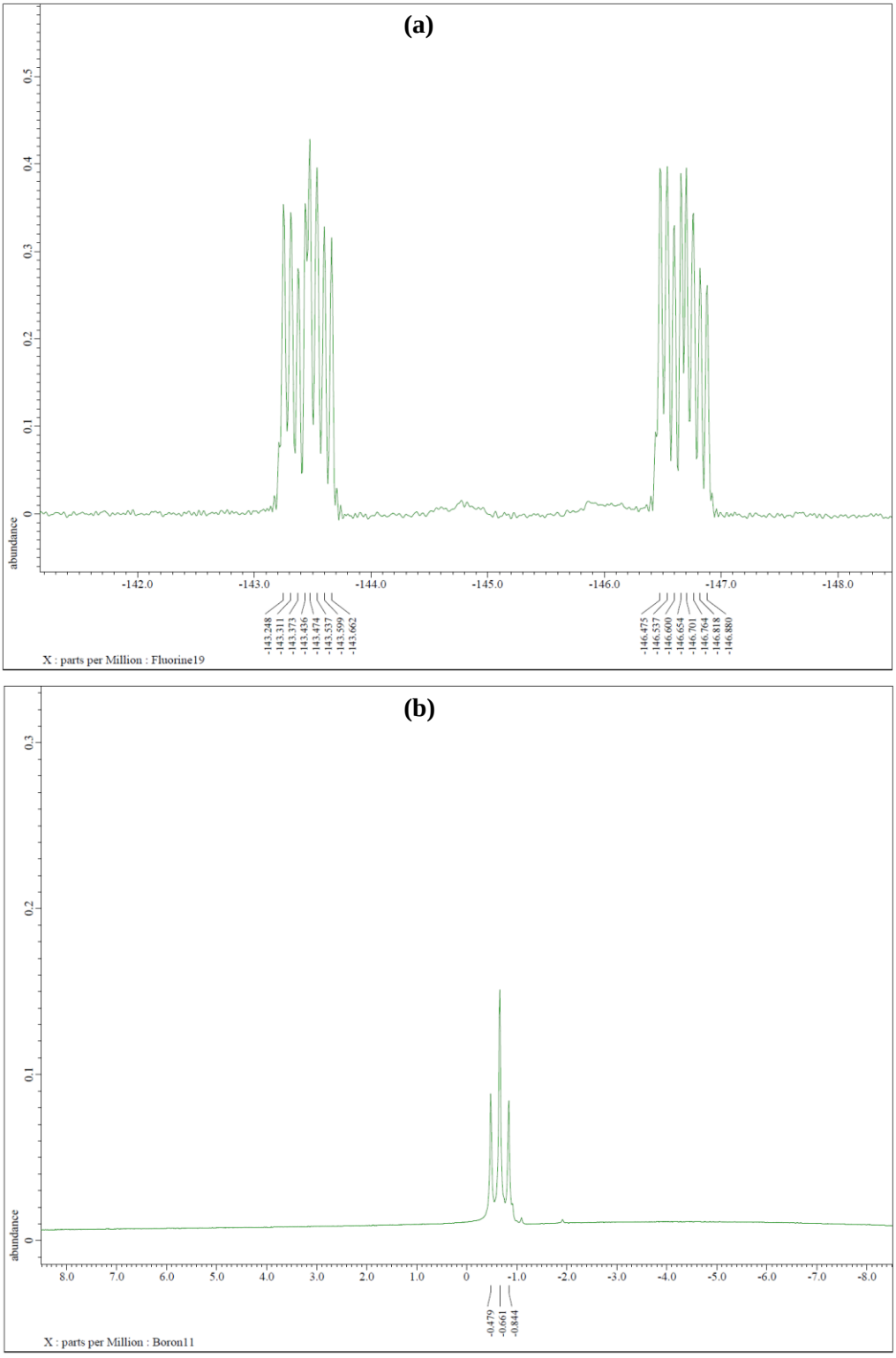

Fig. S10 ^{19}**F** (a) and ^{11}**B** (b) NMR spectra of **HPIB1** in $CDCl_3$

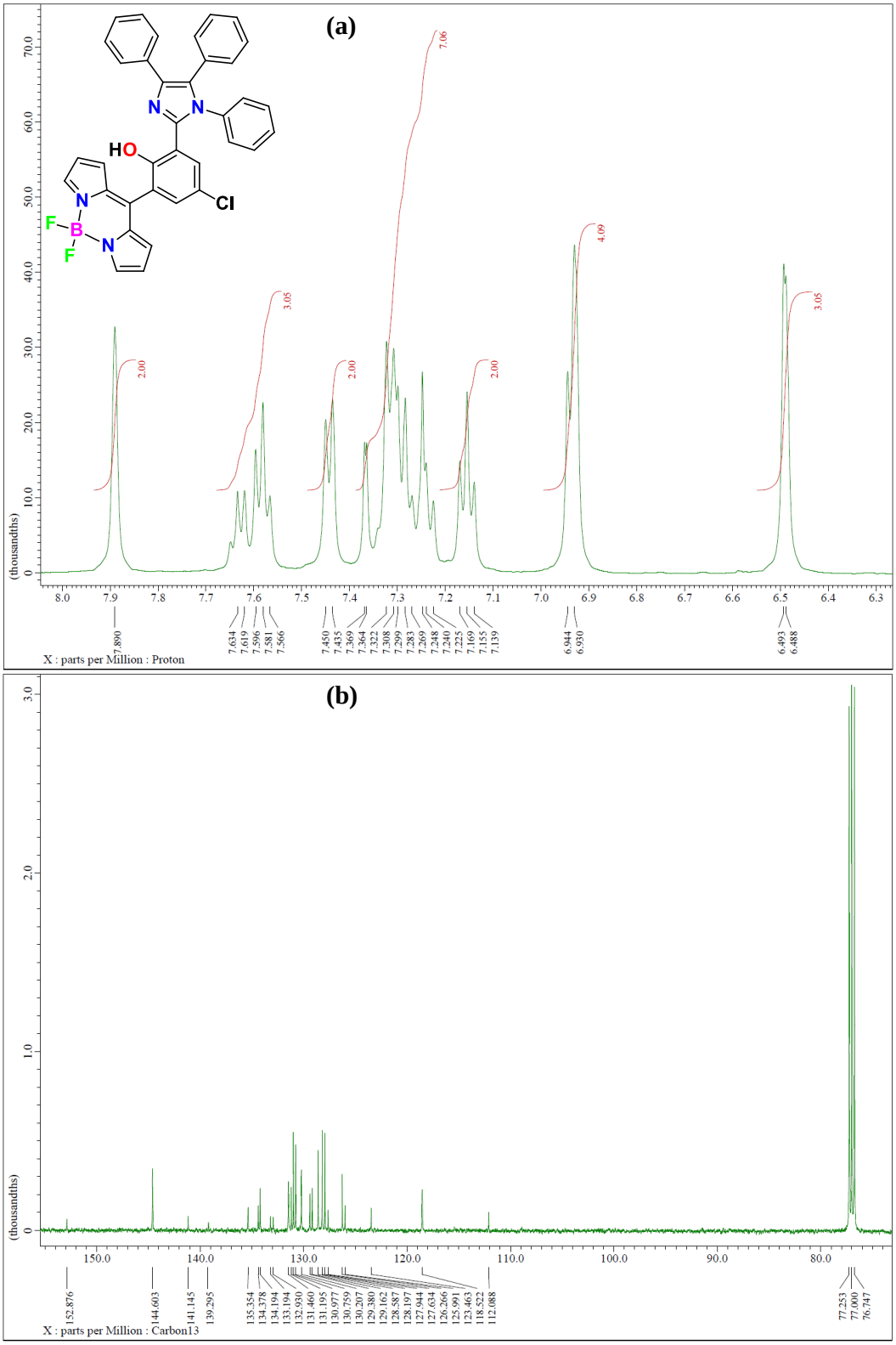

Fig. S11 **^{1}H** (a) and **^{13}C** (b) NMR spectra of **HPIB2** in $CDCl_3$

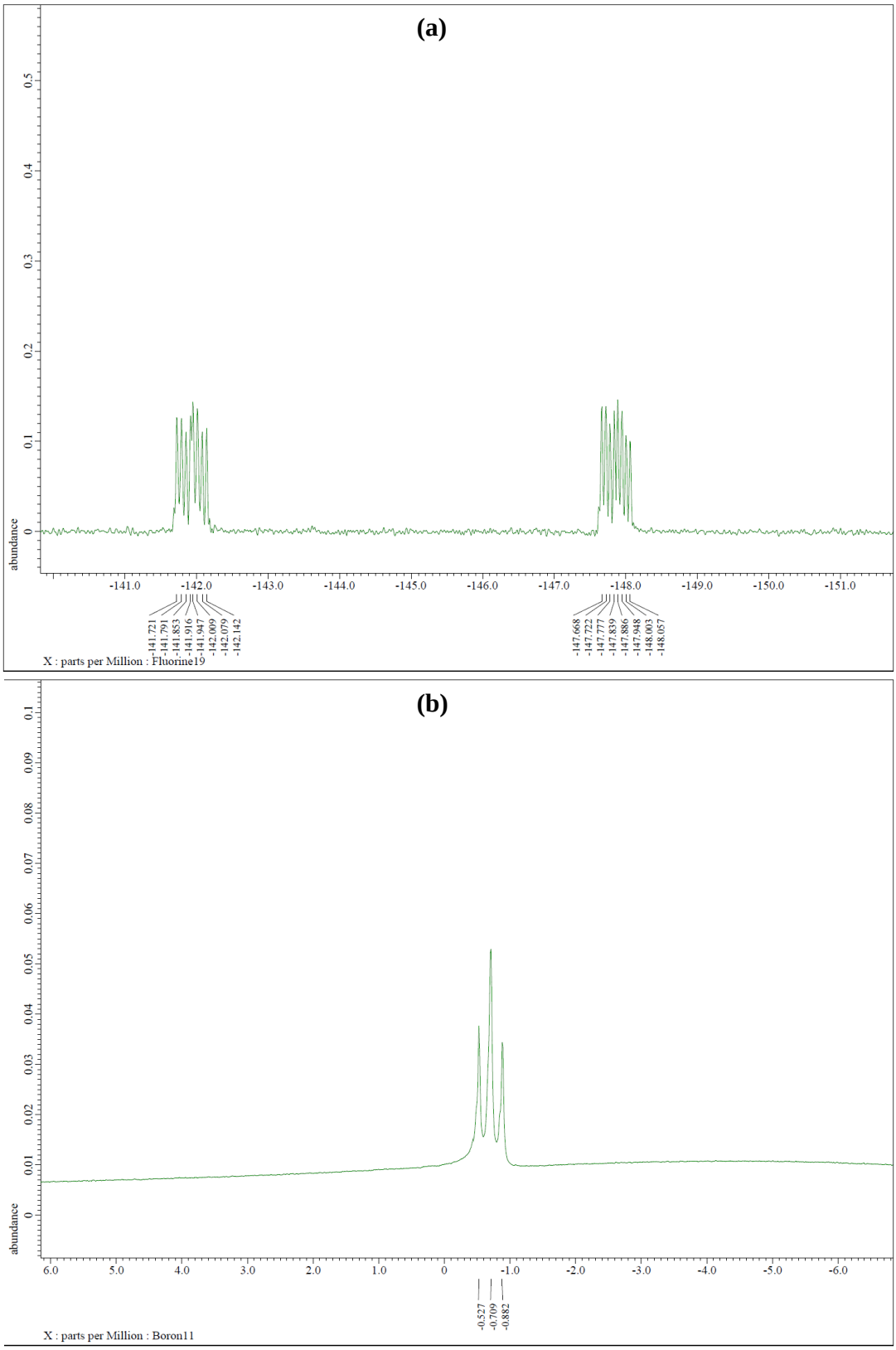

Fig. S12 **^{19}F** (a) and **^{11}B** (b) NMR spectra of **HPIB2** in $CDCl_3$

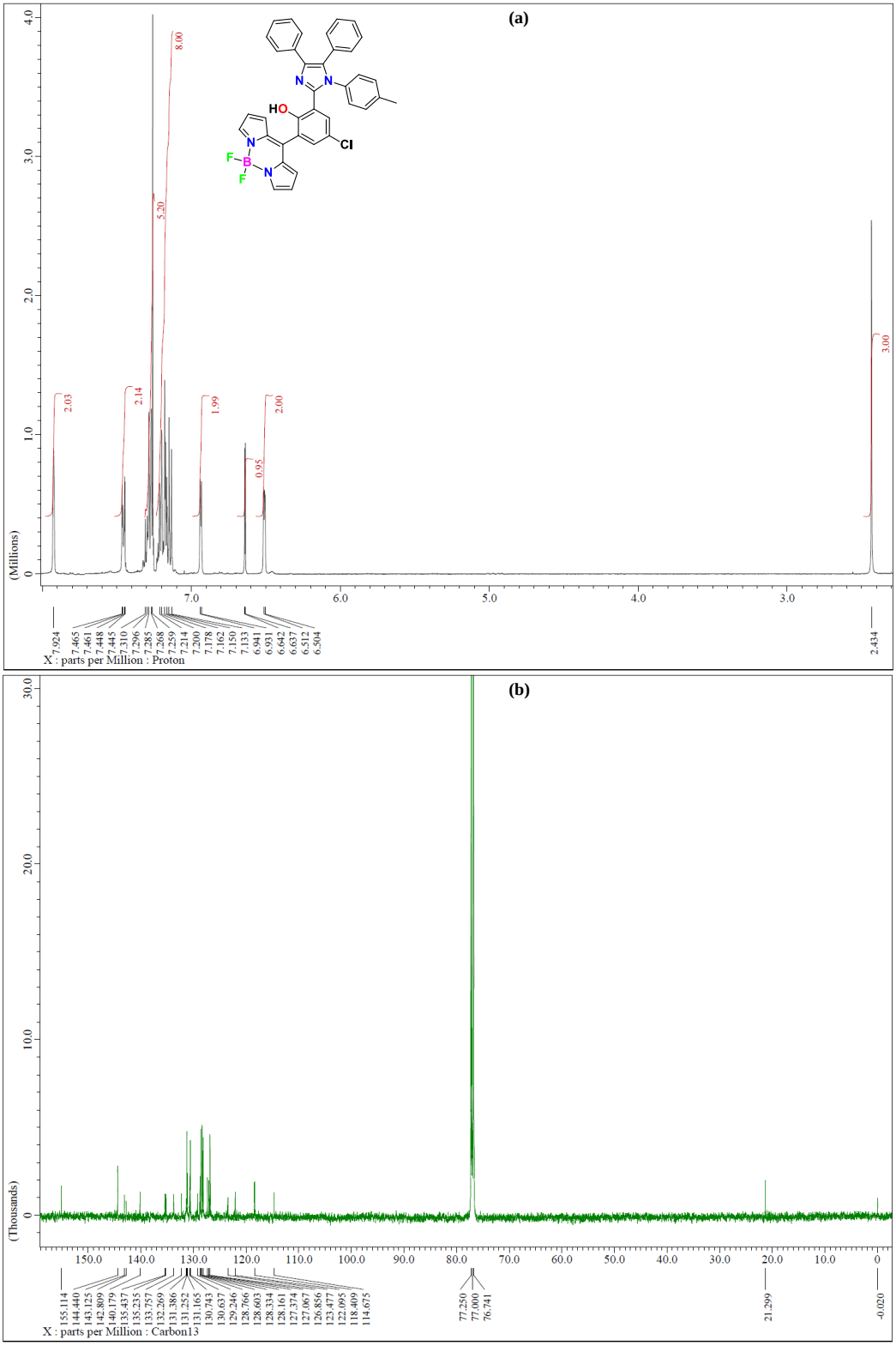

Fig. S13 **^{1}H** (a) and **^{13}C** (b) NMR spectra of **HPIB3** in $CDCl_3$

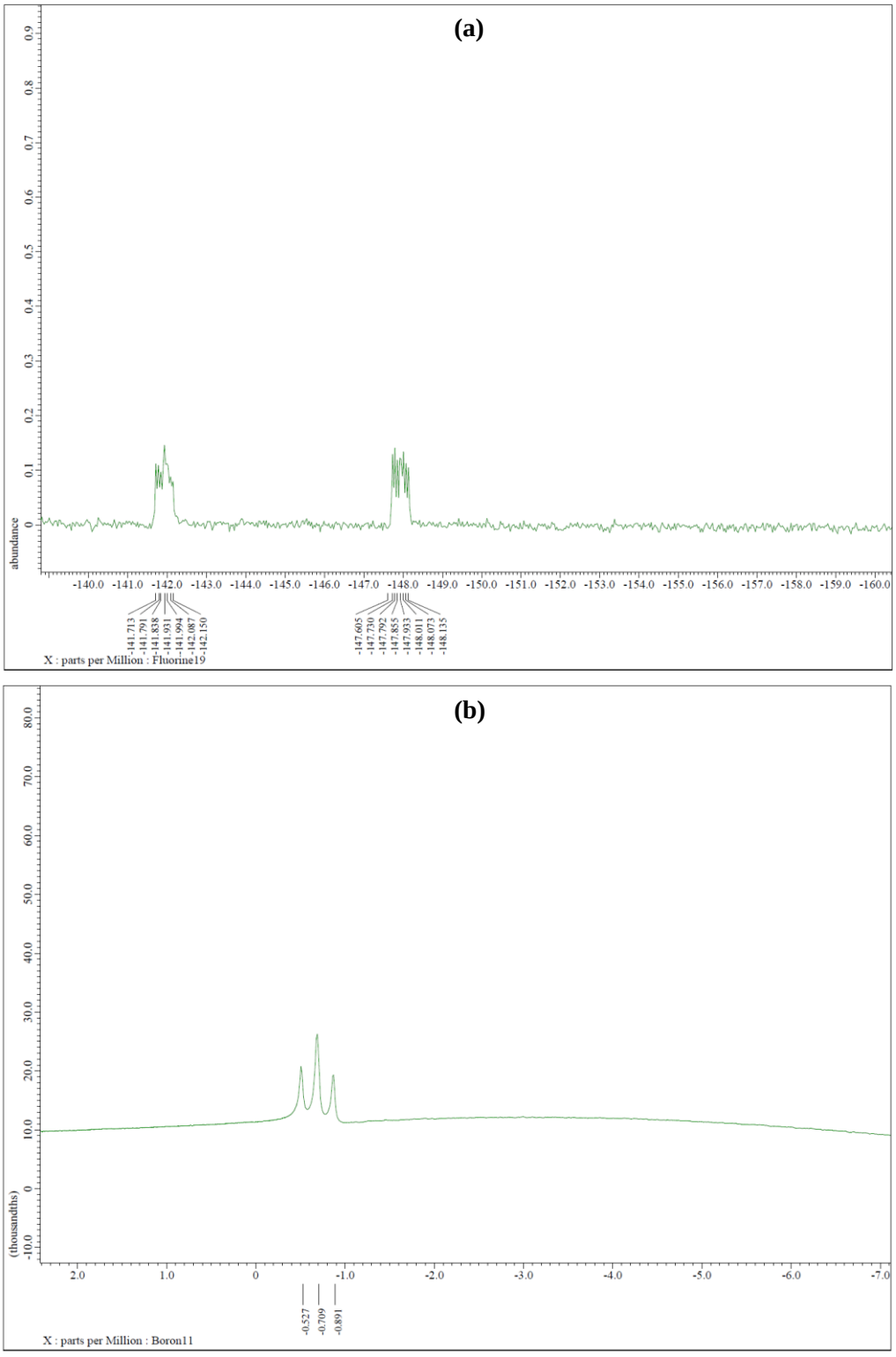

Fig. S14 ^{19}**F** (a) and ^{11}**B** (b) NMR spectra of **HPIB3** in $CDCl_3$.

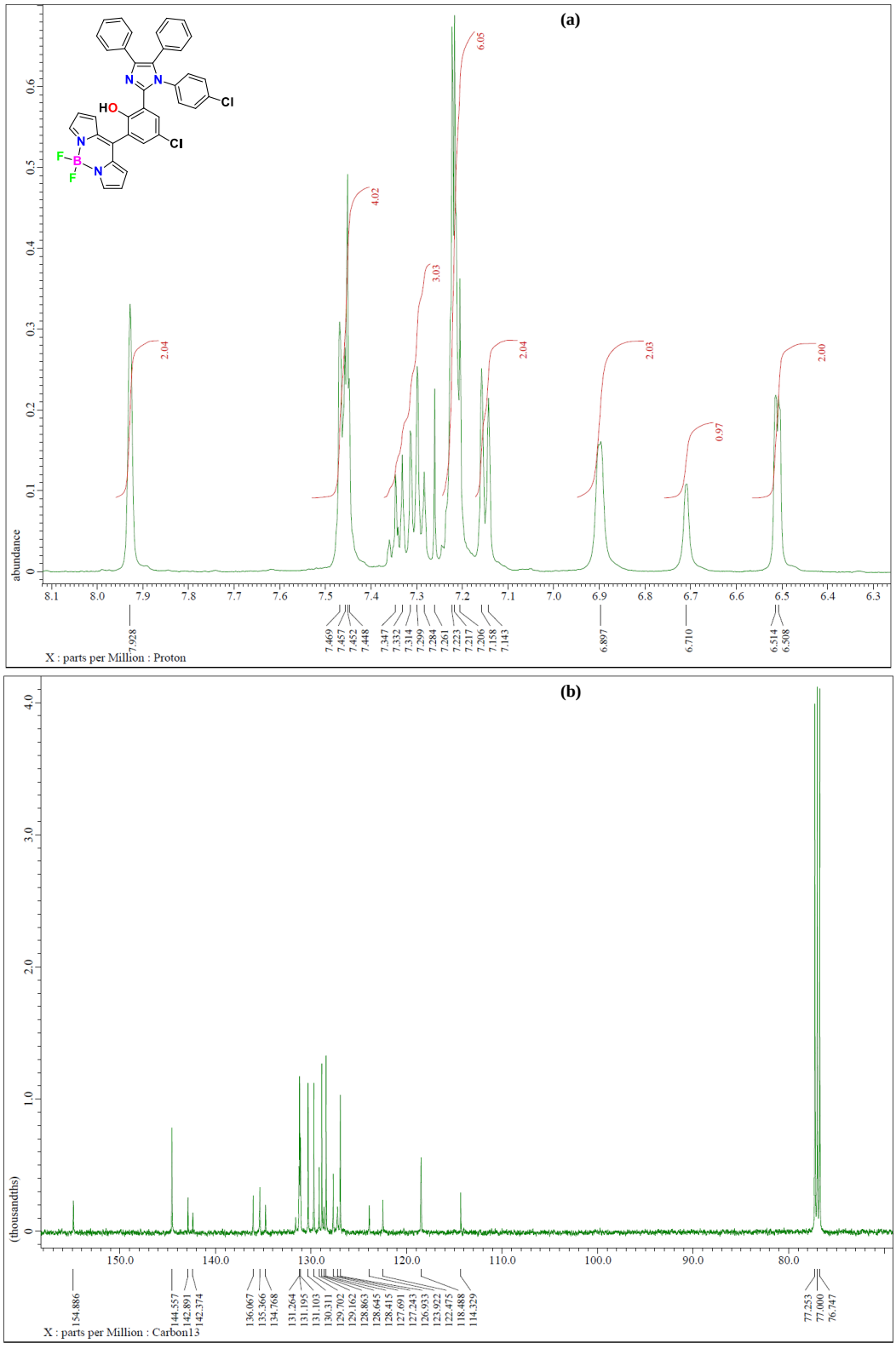

Fig. S15 **^{1}H** (a) and **^{13}C** (b) NMR spectra of **HPIB4** in $CDCl_3$.

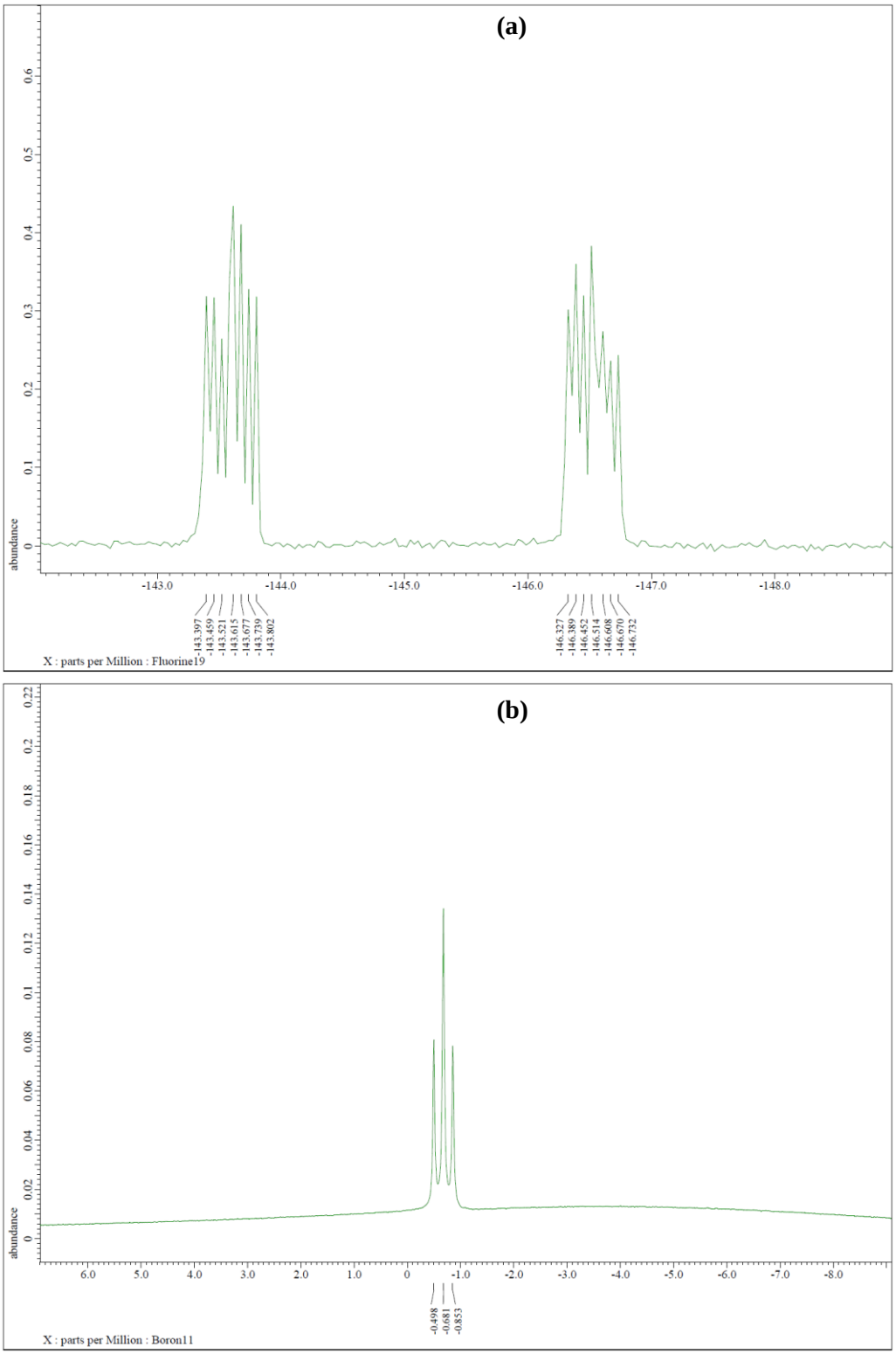

Fig. S16 ^{19}**F** (a) and ^{11}**B** (b) NMR spectra of **HPIB4** in $CDCl_3$.

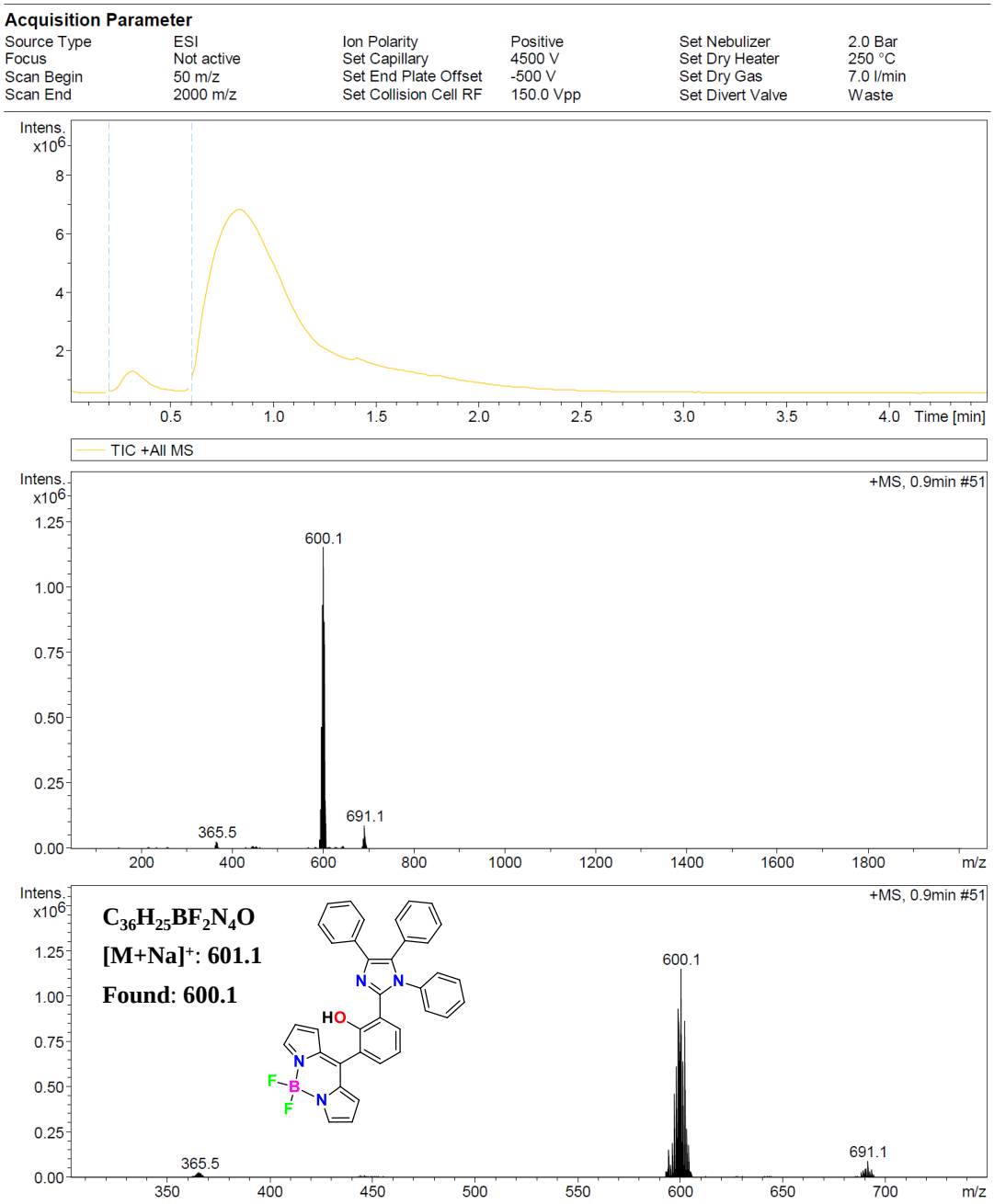

Fig. S17 ESI-MS spectra of **HPIB1**.

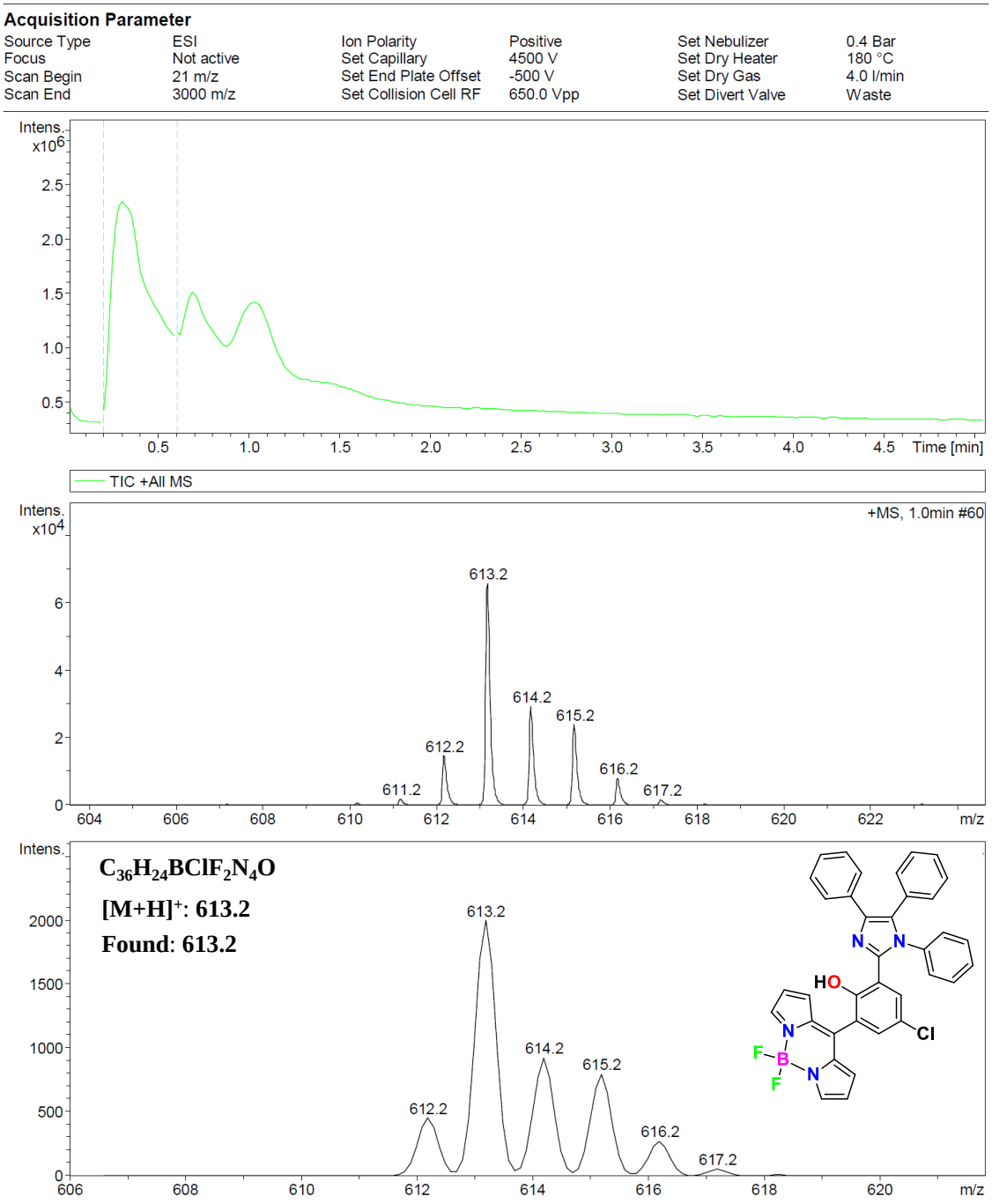

Fig. S18 ESI-MS spectra of **HPIB2**.

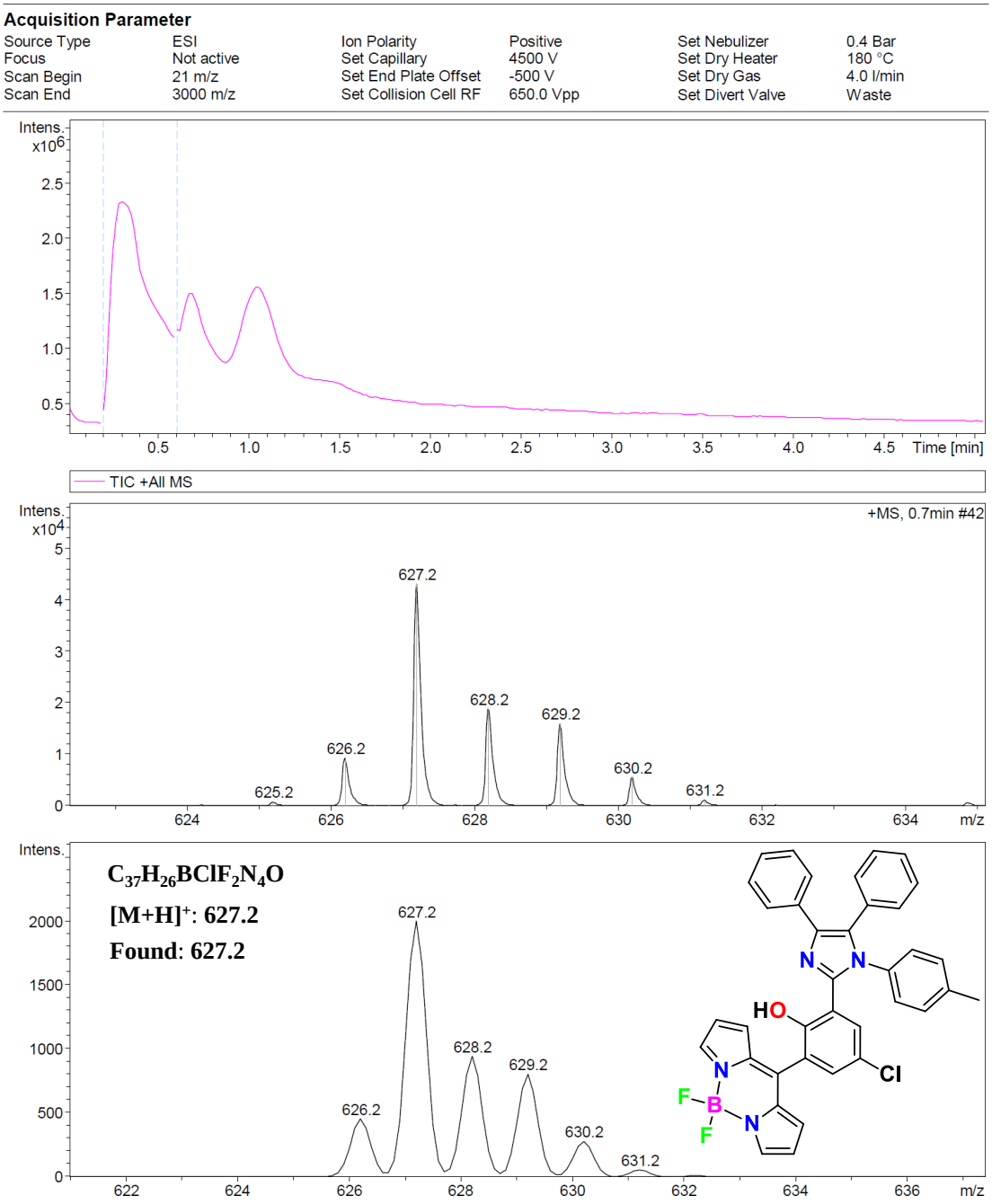

Fig. S19 ESI-MS spectra of **HPIB3**.

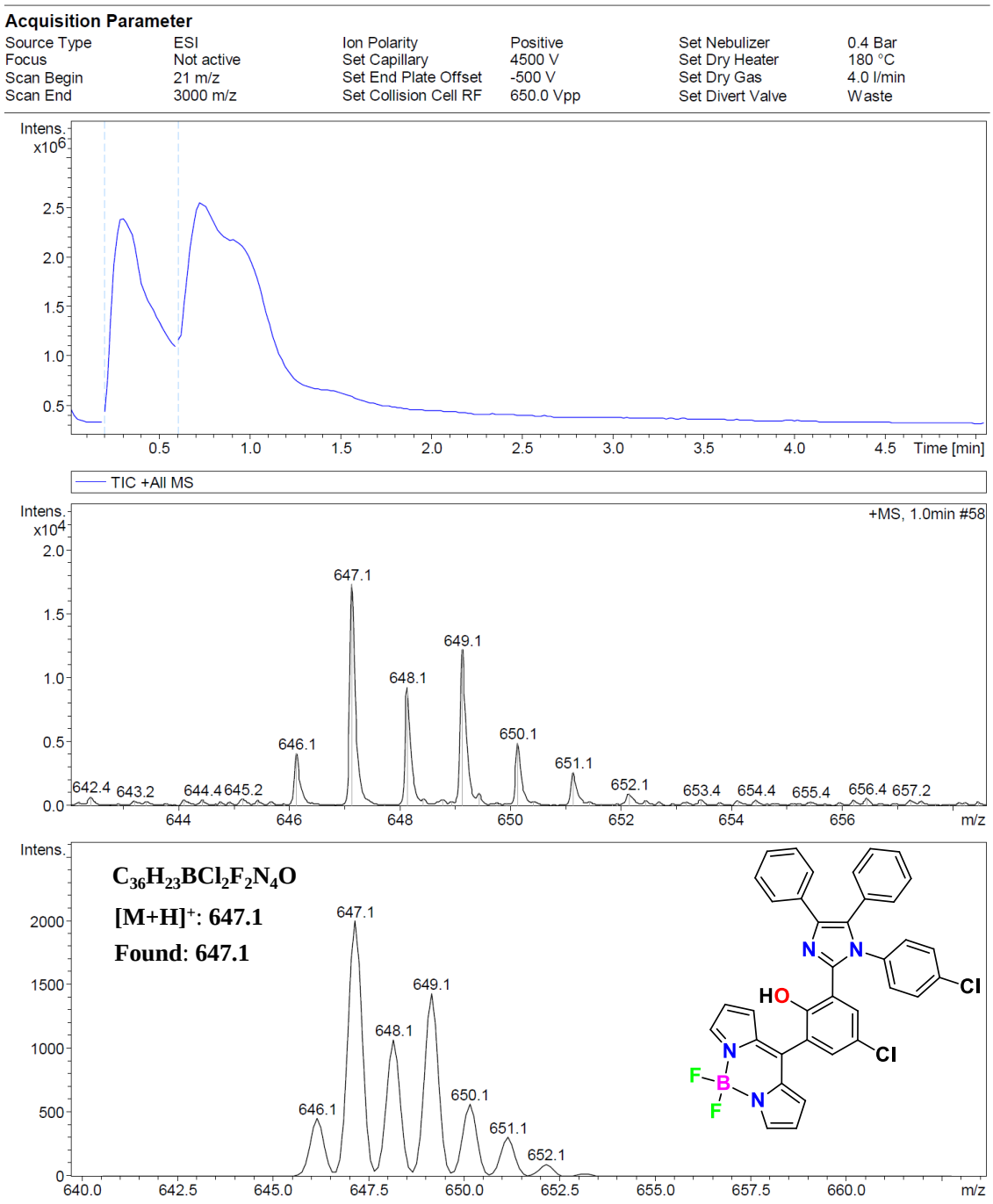

Fig. S20 ESI-MS spectra of **HPIB4**.

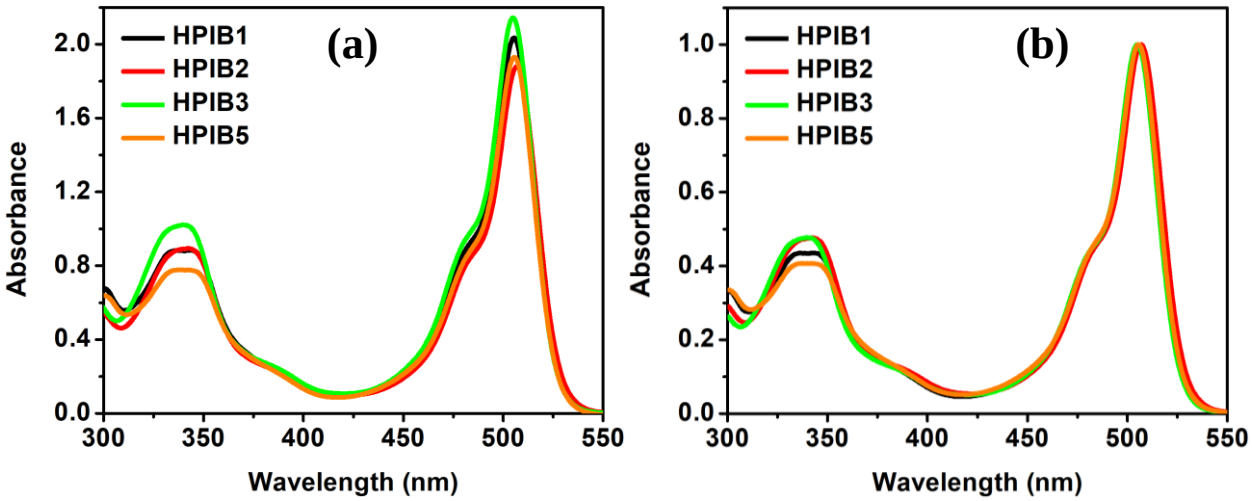

Fig. S21 Absorption spectra (a) and its normalized representation (b) for **HPIB1**–**HPIB4** (c; 50 μM, DMF).

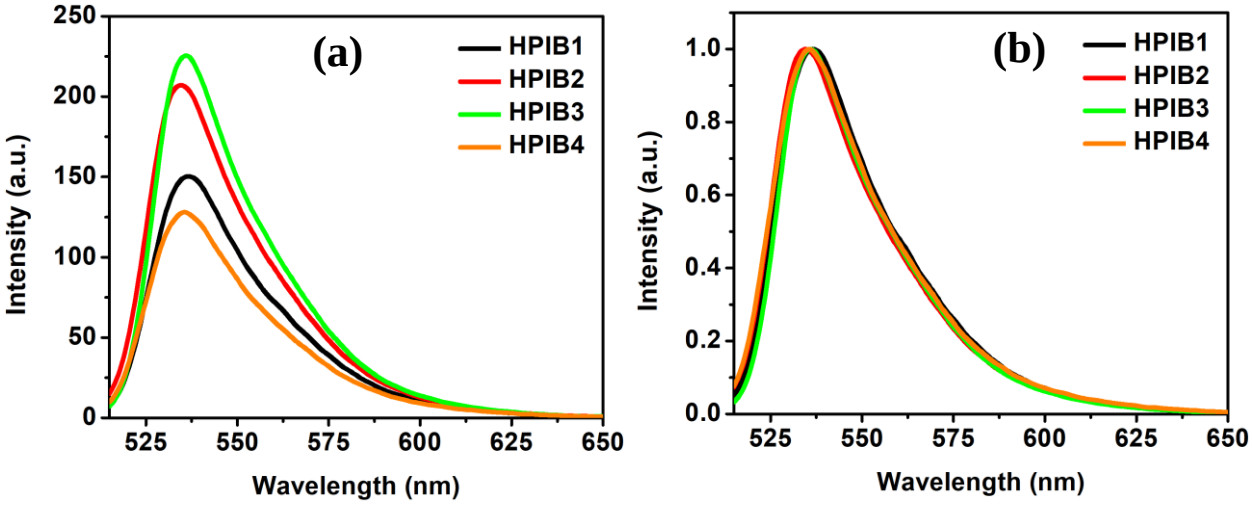

Fig. S22 Emission spectra (a) and its normalized representation (b) for **HPIB1**–**HPIB4** (c; 50 μM, DMF, λ_{ex}; 505 nm).

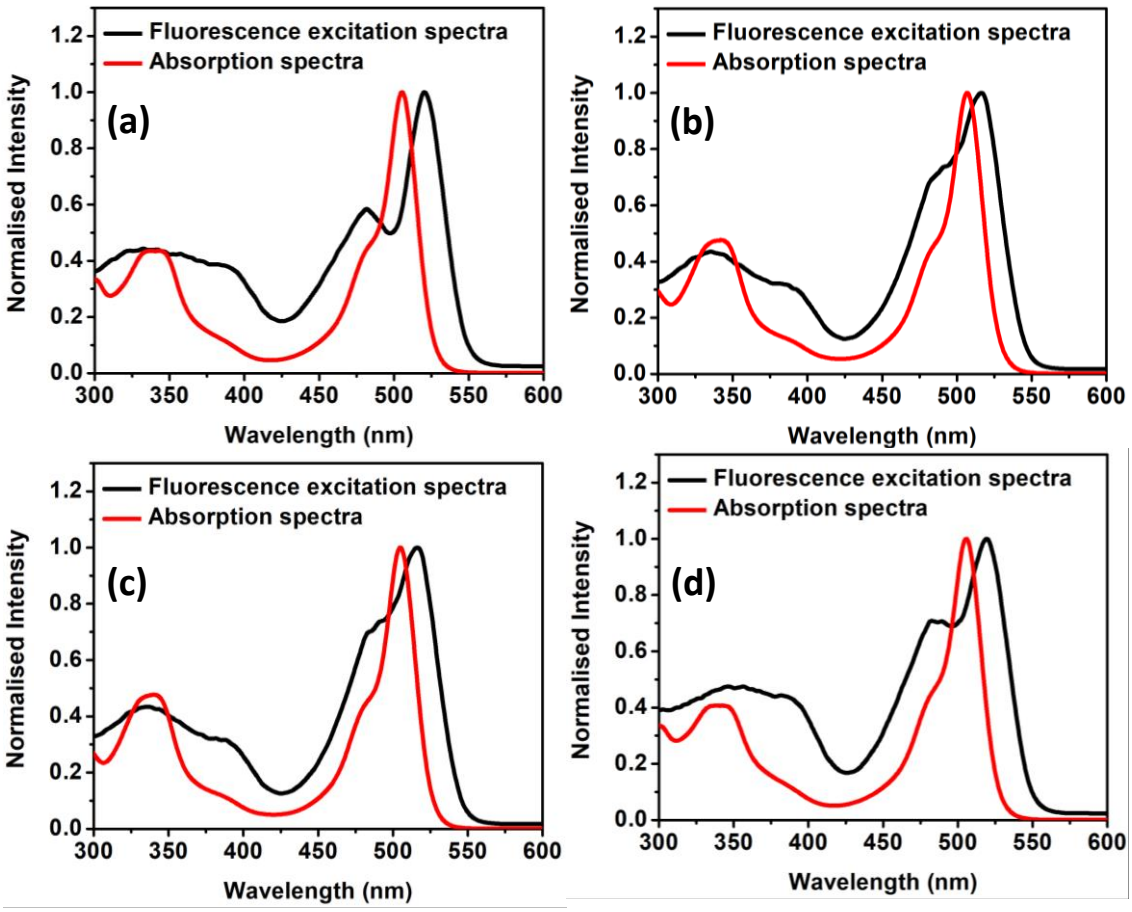

Fig. S23 Fluorescence excitation spectra and their comparison with absorption spectra for **HPIB1** (a), **HPIB2** (b), **HPIB3** (c), and **HPIB4** (d) (c; 50 μM, DMF).

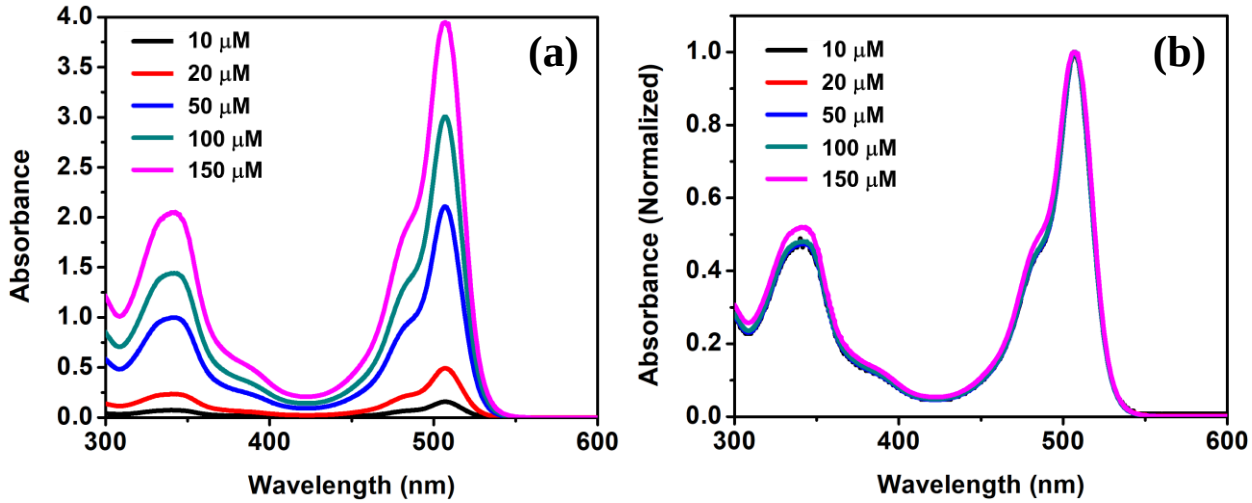

Fig. S24 Absorption spectra (a) with varying compound concentration and normalized representation (b) in DMF for **HPIB1**.

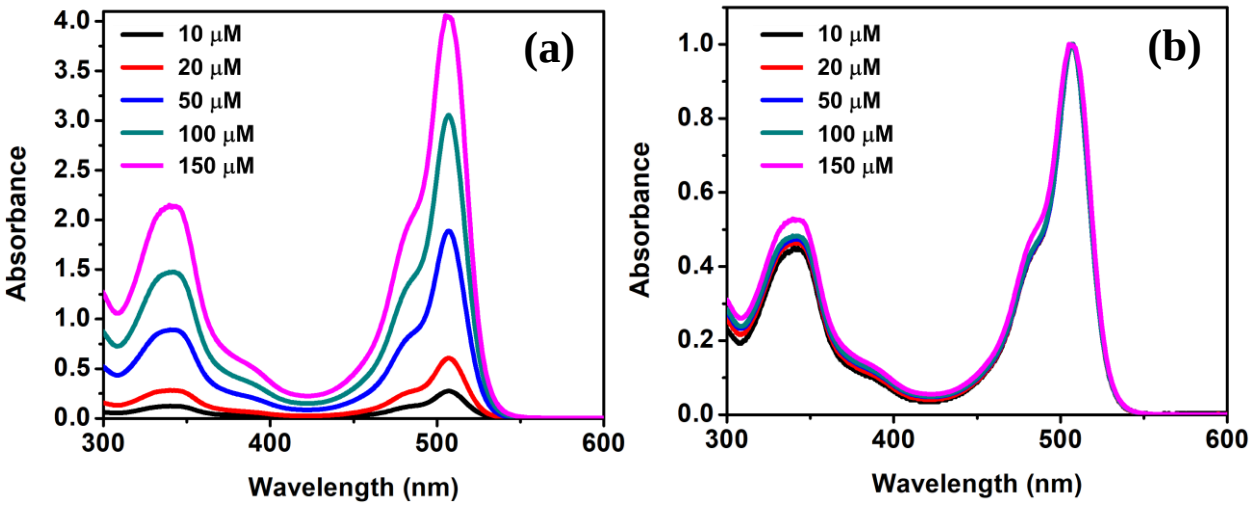

Fig. S25 Absorption spectra (a) with varying compound concentration and normalized representation (b) in DMF for **HPIB2**.

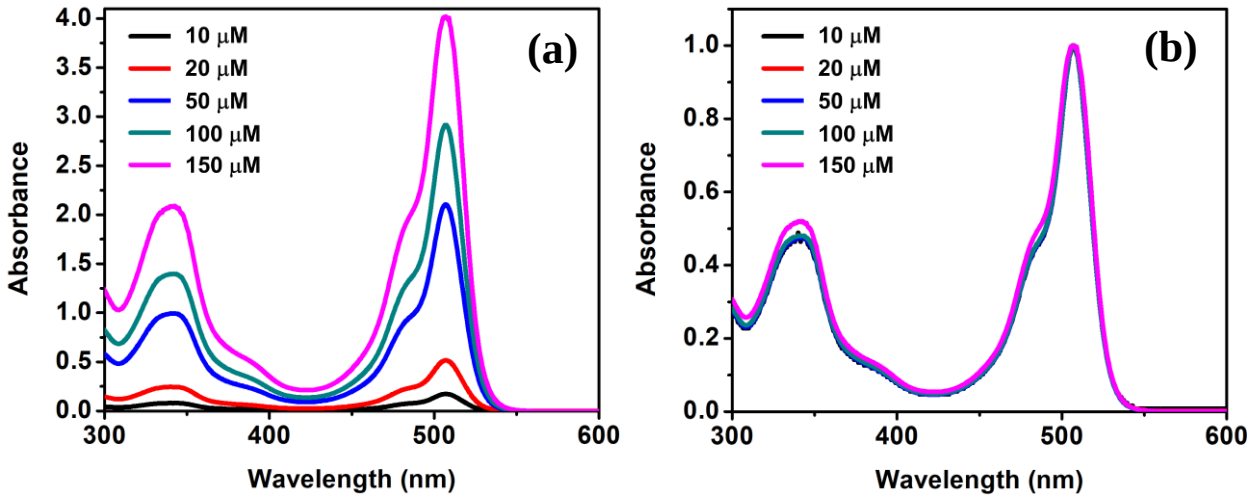

Fig. S26 Absorption spectra (a) with varying compound concentration and normalized representation (b) in DMF for **HPIB3**.

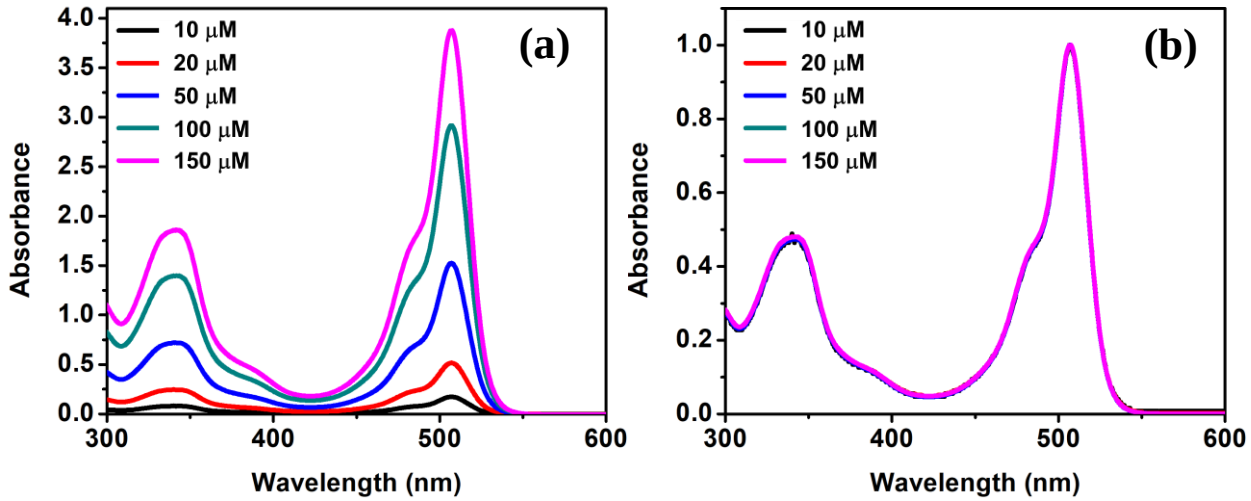

Fig. S27 Absorption spectra (a) with varying compound concentration and normalized representation (b) in DMF for **HPIB4**.

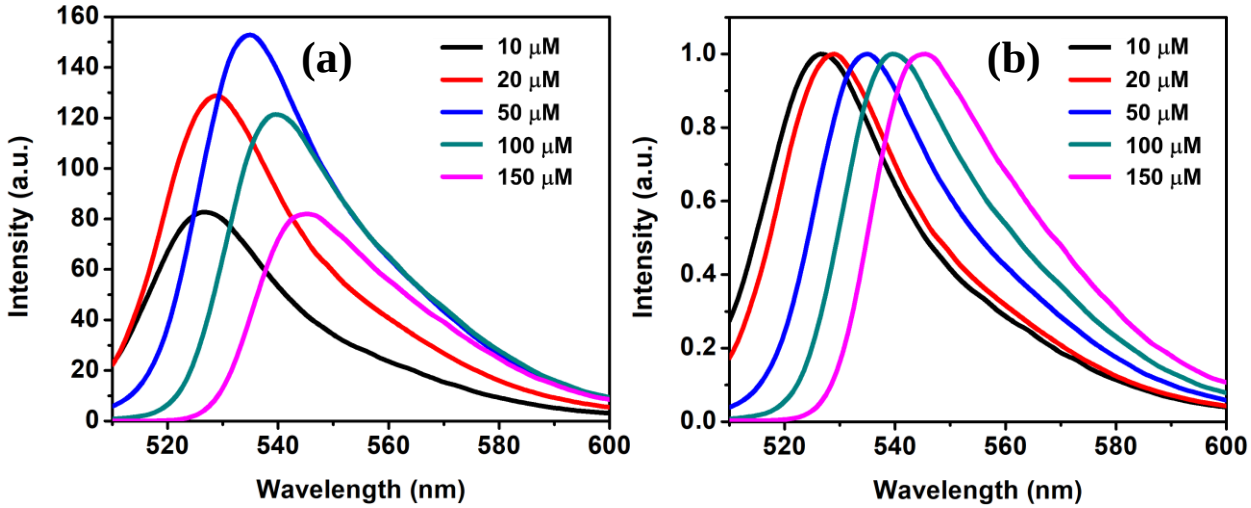

Fig. S28 Emission spectra (a) with varying compound concentration and normalized representation (b) in DMF for **HPIB1**.

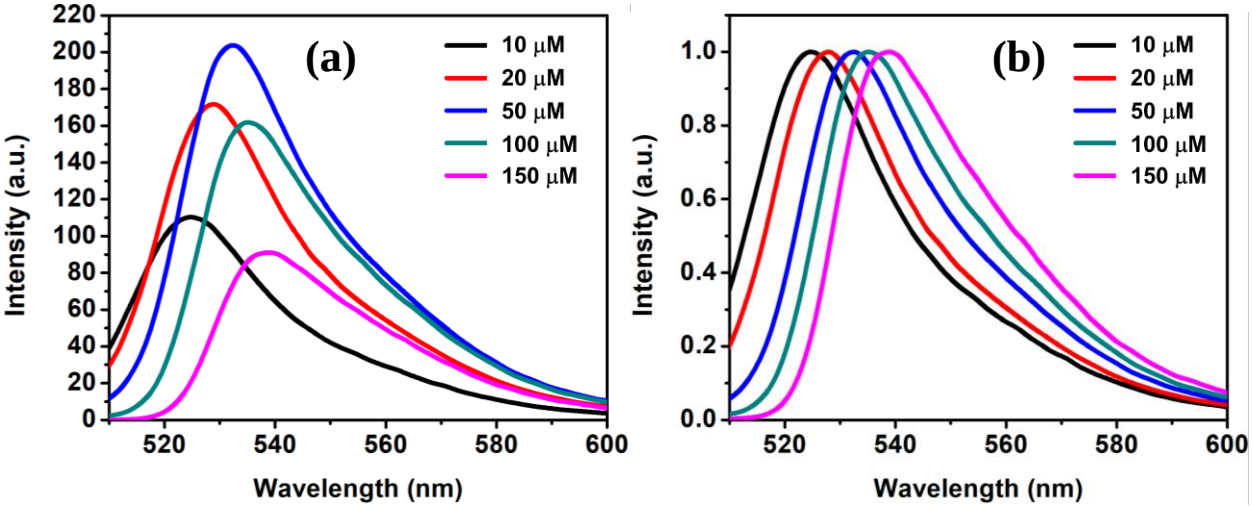

Fig. S29 Emission spectra (a) with varying compound concentration and normalized representation (b) in DMF for **HPIB2**.

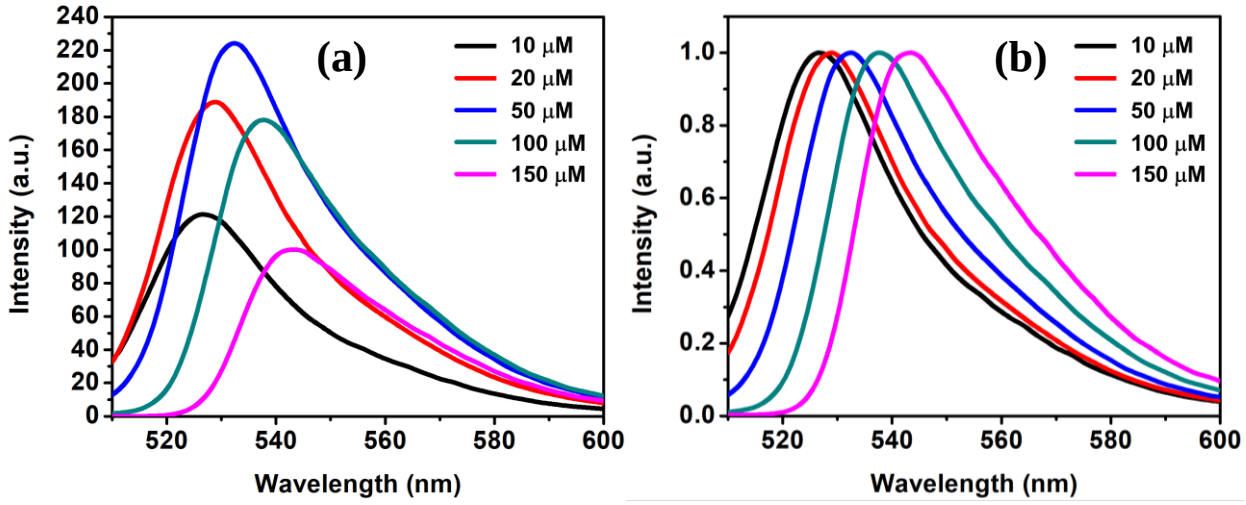

Fig. S30 Emission spectra (a) with varying compound concentration and normalized representation (b) in DMF for **HPIB3**.

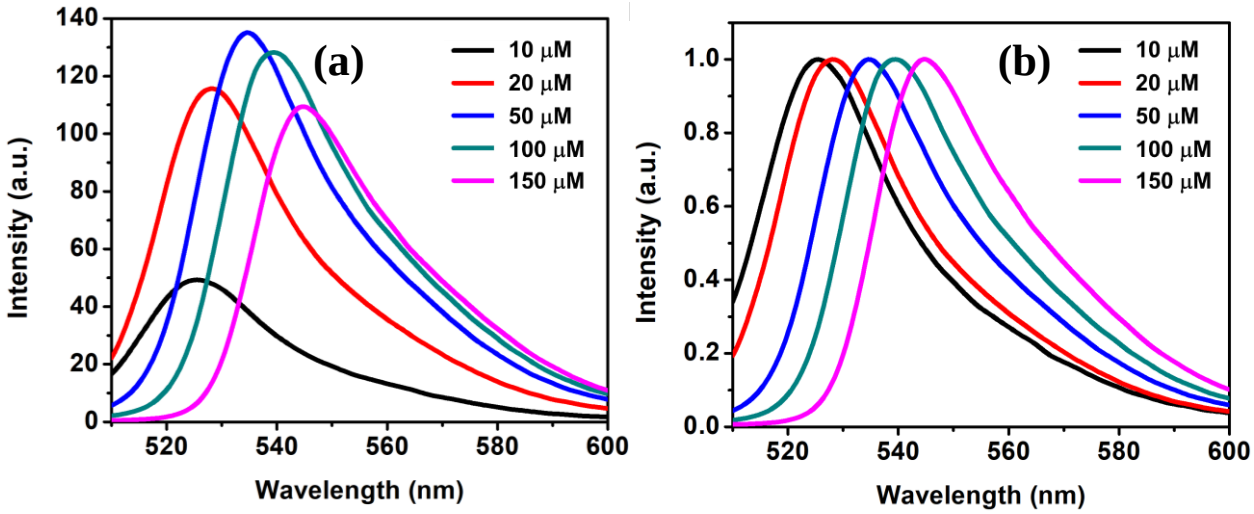

Fig. S31 Emission spectra (a) with varying compound concentration and normalized representation (b) in DMF for **HPIB4**.

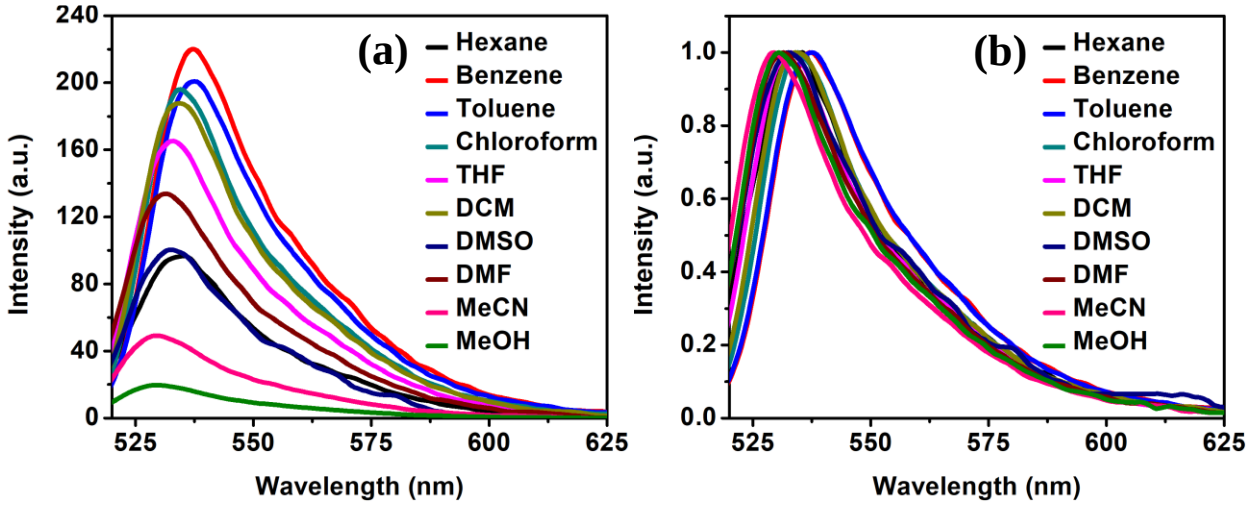

Fig. S32 Emission spectra (a) and normalized representation (b) in different solvents with varying polarities for **HPIB1** (c; 50 μM).

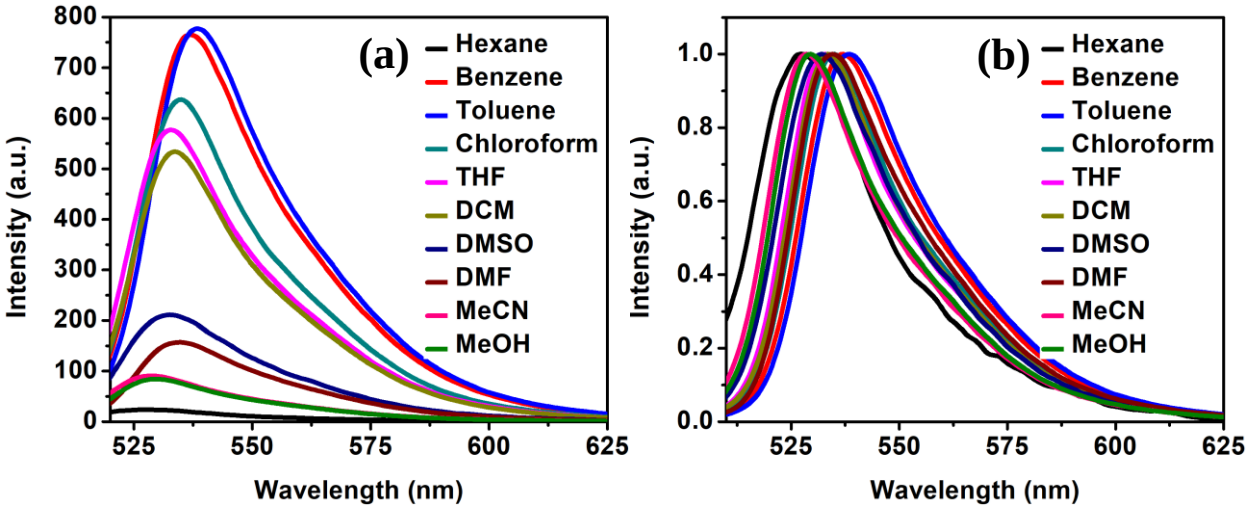

Fig. S33 Emission spectra (a) and normalized representation (b) in different solvents with varying polarities for **HPIB3** (c; 50 μM).

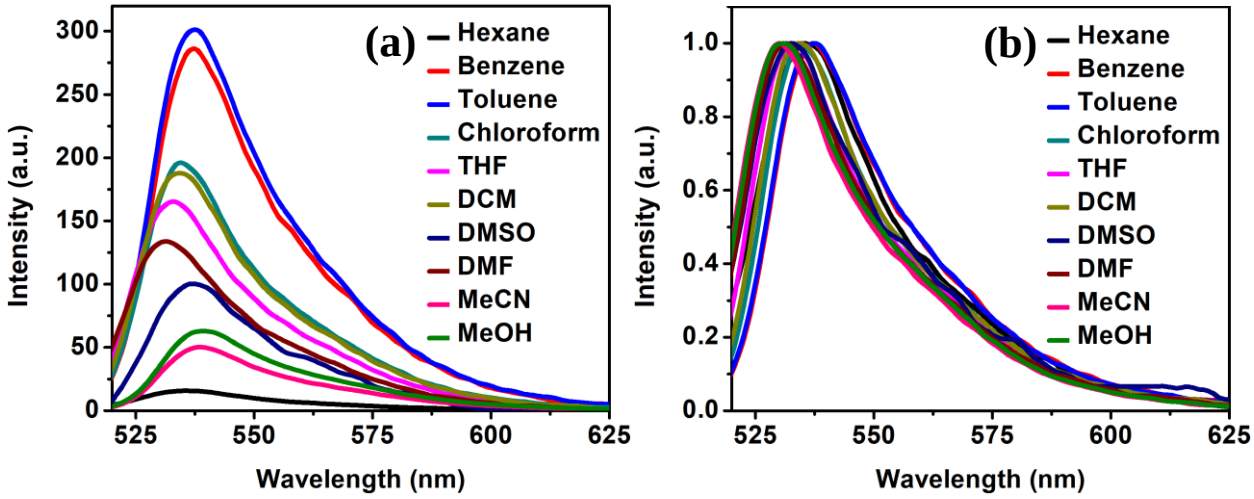

Fig. S34 Emission spectra (a) and normalized representation (b) in different solvents with varying polarities for **HPIB4** (c; 50 μM).

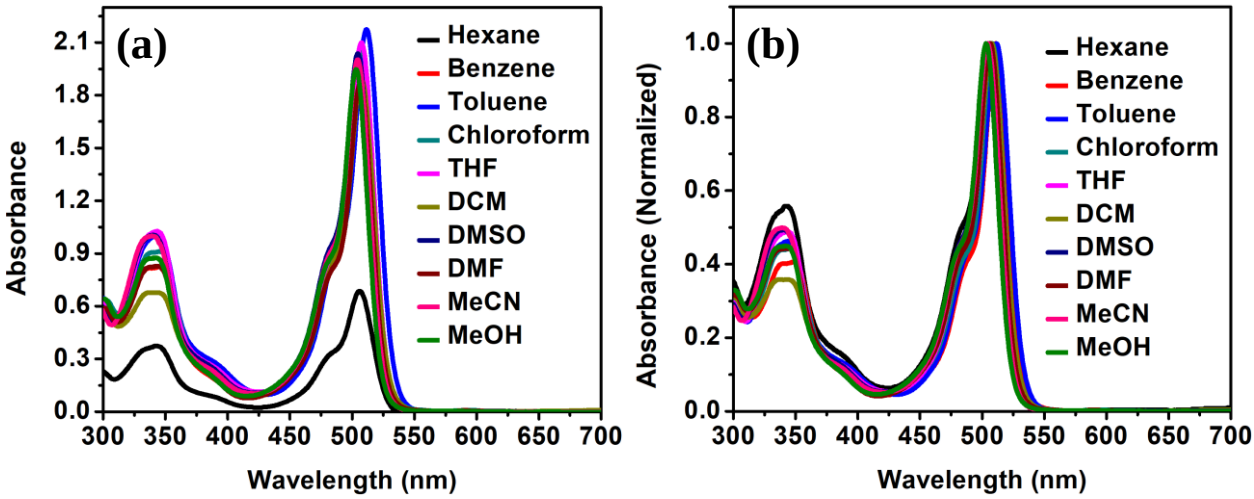

Fig. S35 Absorption spectra (a) and normalized representation (b) in different solvents with varying polarities for **HPIB1** (c; 50 μM).

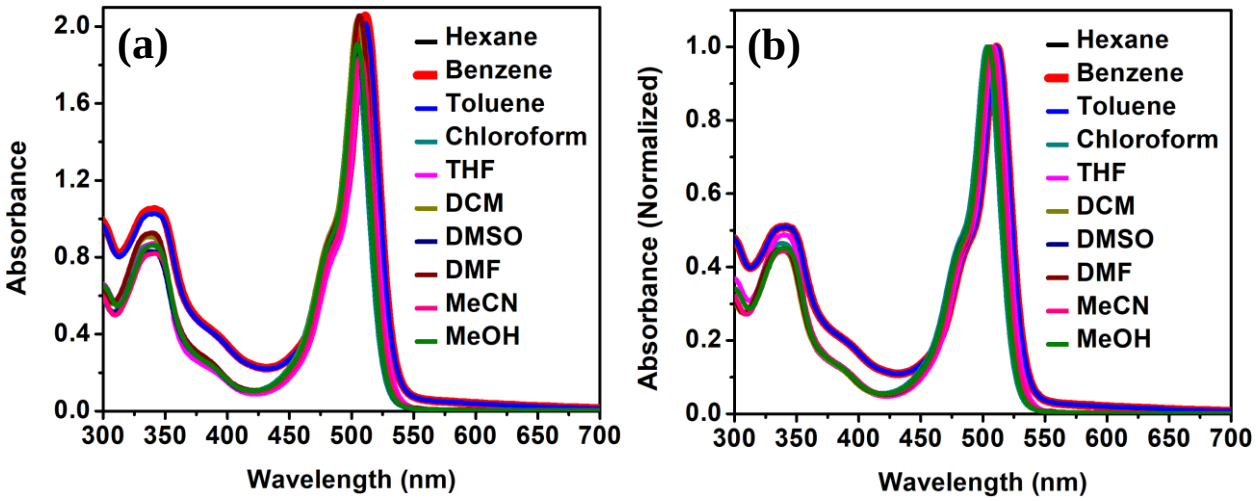

Fig. S36 Absorption spectra (a) and normalized representation (b) in different solvents with varying polarities for **HPIB2** (c; 50 μM).

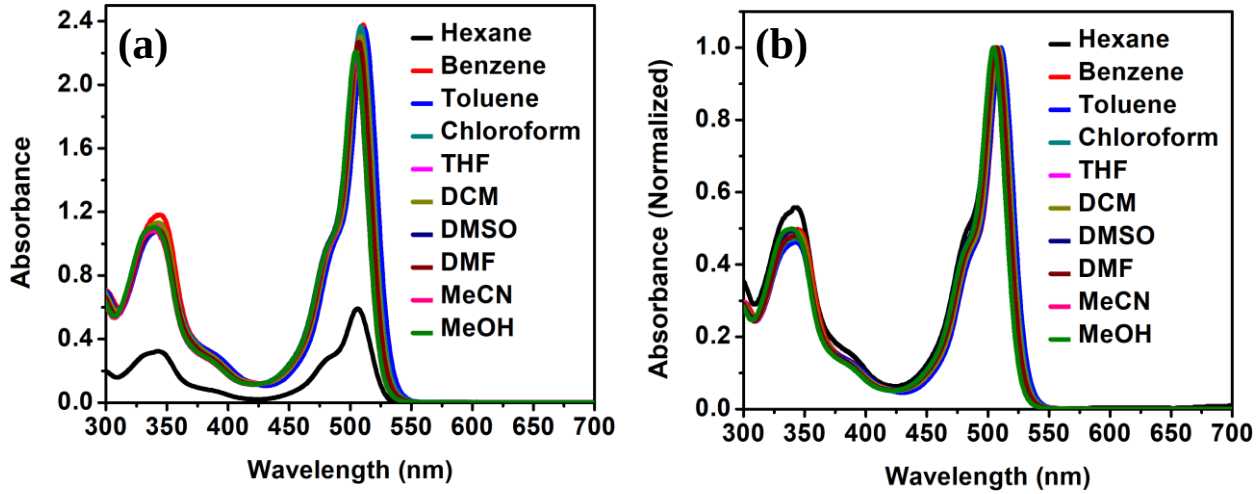

Fig. S37 Absorption spectra (a) and normalized representation (b) in different solvents with varying polarities for **HPIB3** (c; 50 μM).

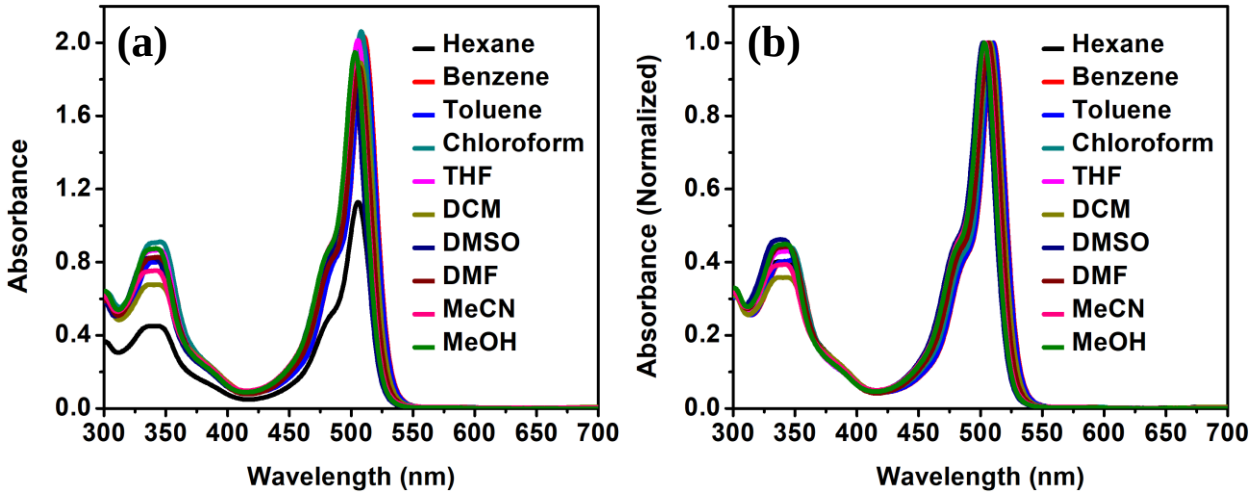

Fig. S38 Absorption spectra (a) and normalized representation (b) in different solvents with varying polarities for **HPIB4** (c; 50 μM).

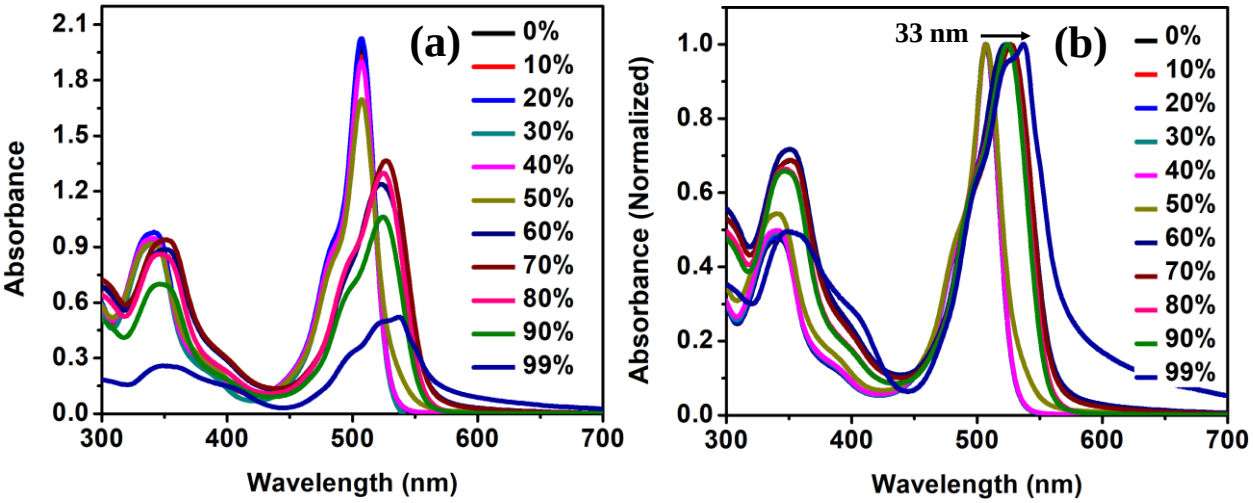

Fig. S39 Absorption spectra (a) and normalized representation (b) in DMF/water mixture with varying water volume fractions for **HPIB2** (c; 50 μM).

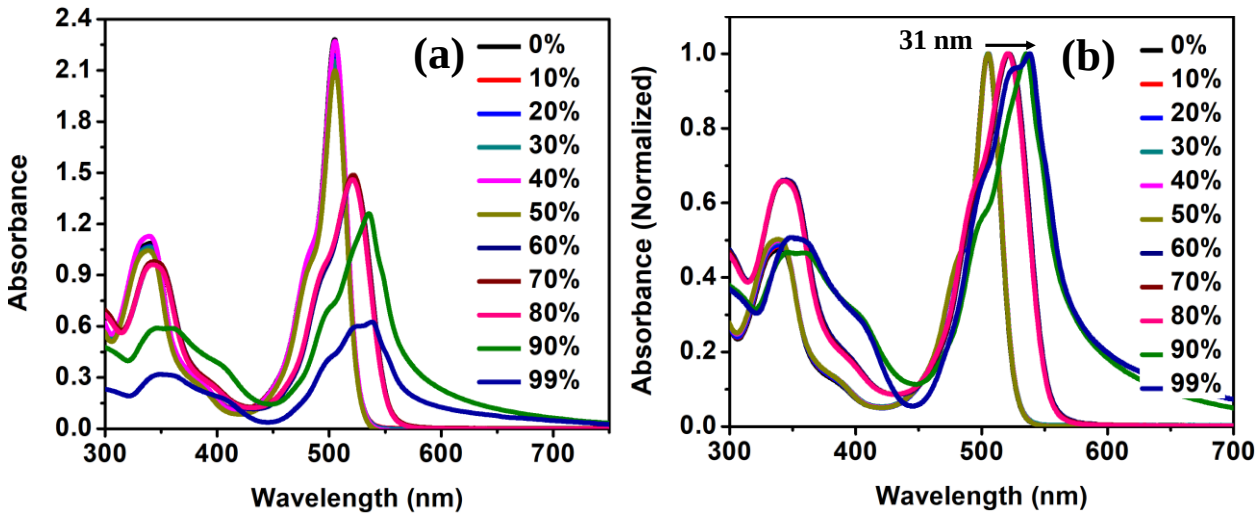

Fig. S40 Absorption spectra (a) and normalized representation (b) in DMF/water mixture with varying water volume fractions for **HPIB3** (c; 50 μM).

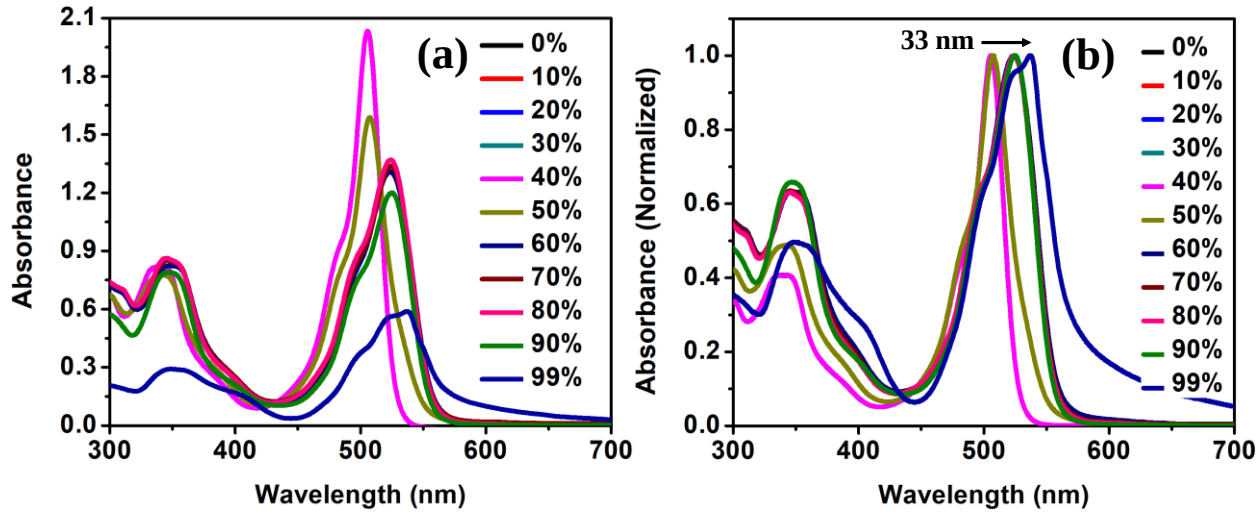

Fig. S41 Absorption spectra (a) and normalized representation (b) in DMF/water mixture with varying water volume fractions for **HPIB4** (c; 50 μM).

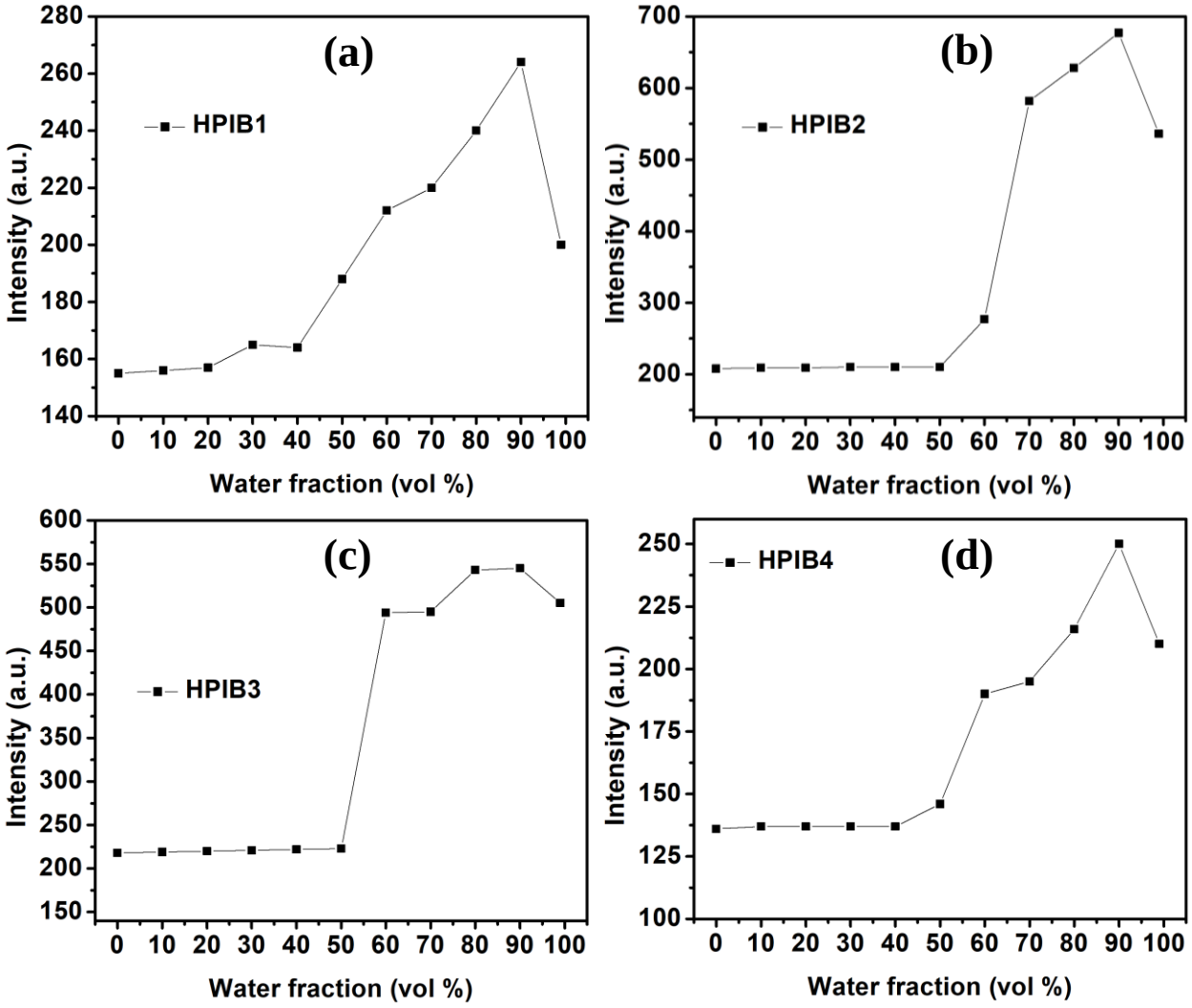

Fig. S42 Variation in emission intensity in DMF/water mixture with varying water volume fractions for **HPIB1**–**HPIB4** (c; 50 μM).

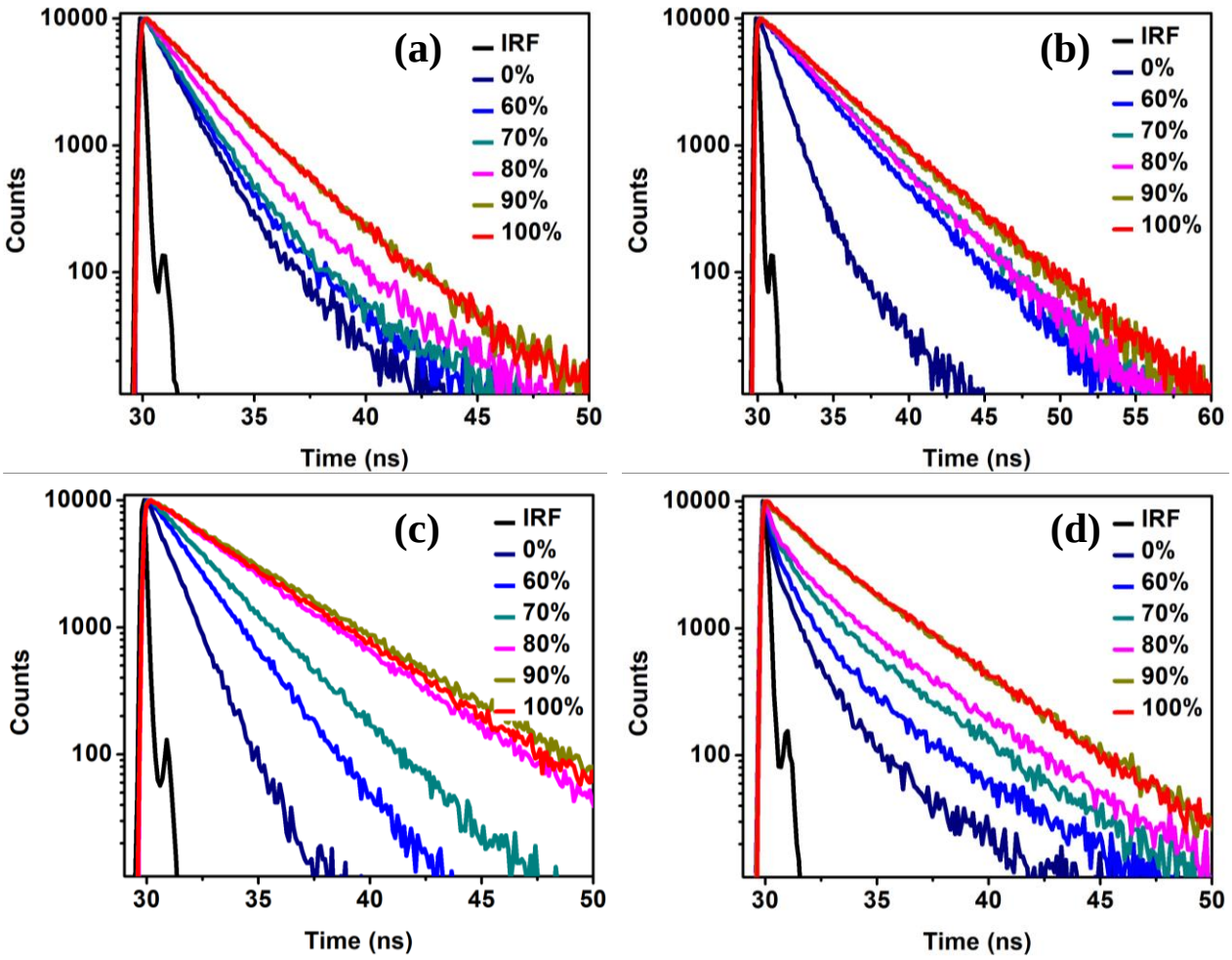

Fig. S43 Time-resolved fluorescence decay profile (λ_{ex} = 482 nm) for **HPIB1** (a), **HPIB2** (b), **HPIB3** (c) and **HPIB4** (d) in DMF/water mixture with varying water volume fractions (c; 50 μM).

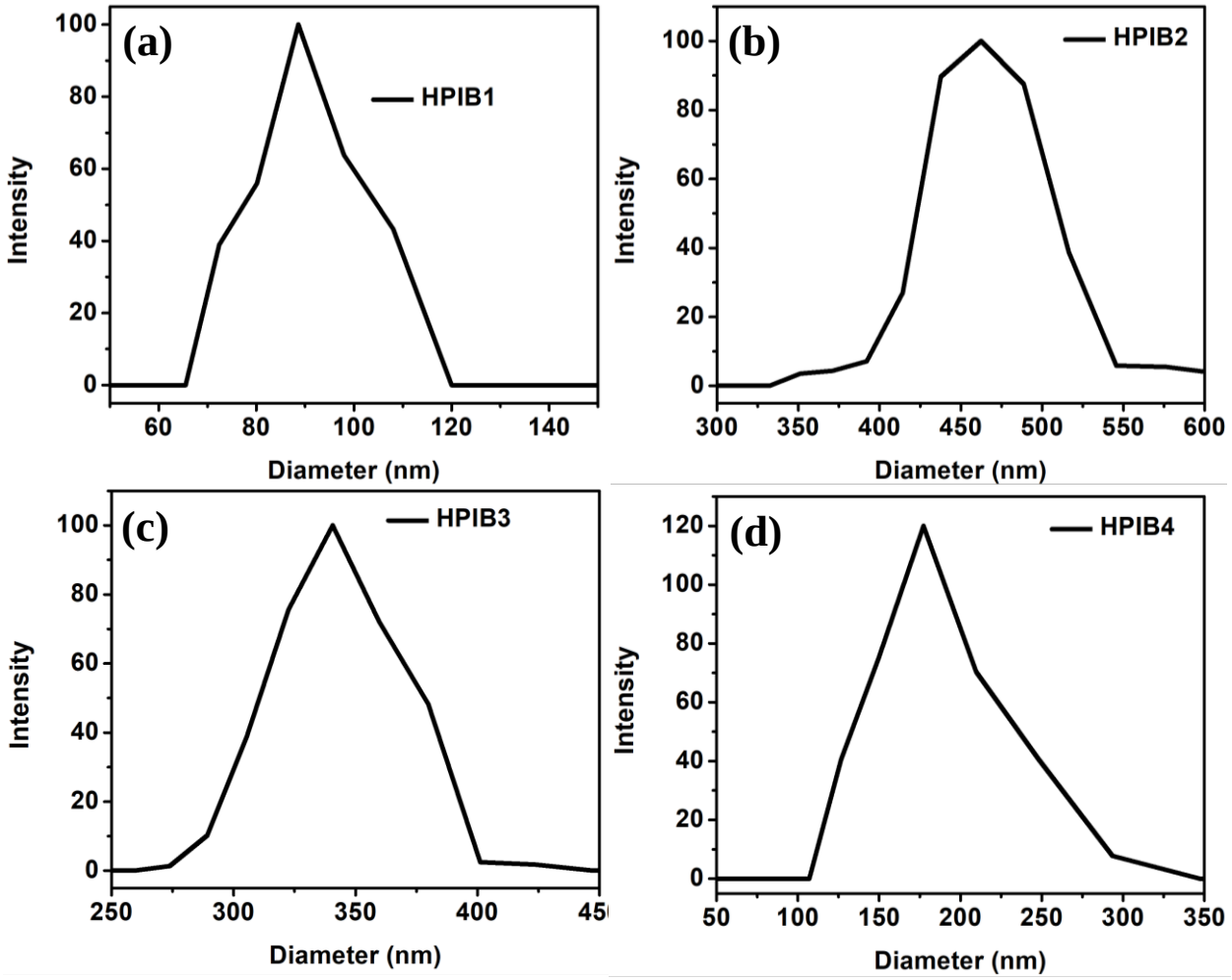

Fig. S44 Dynamic light scattering (DLS) spectra of aggregates for **HPIB1** (a), **HPIB2** (b), **HPIB3** (c), and **HPIB4** (d) in DMF/water mixture at f_w of 99% (c; 50 μM).

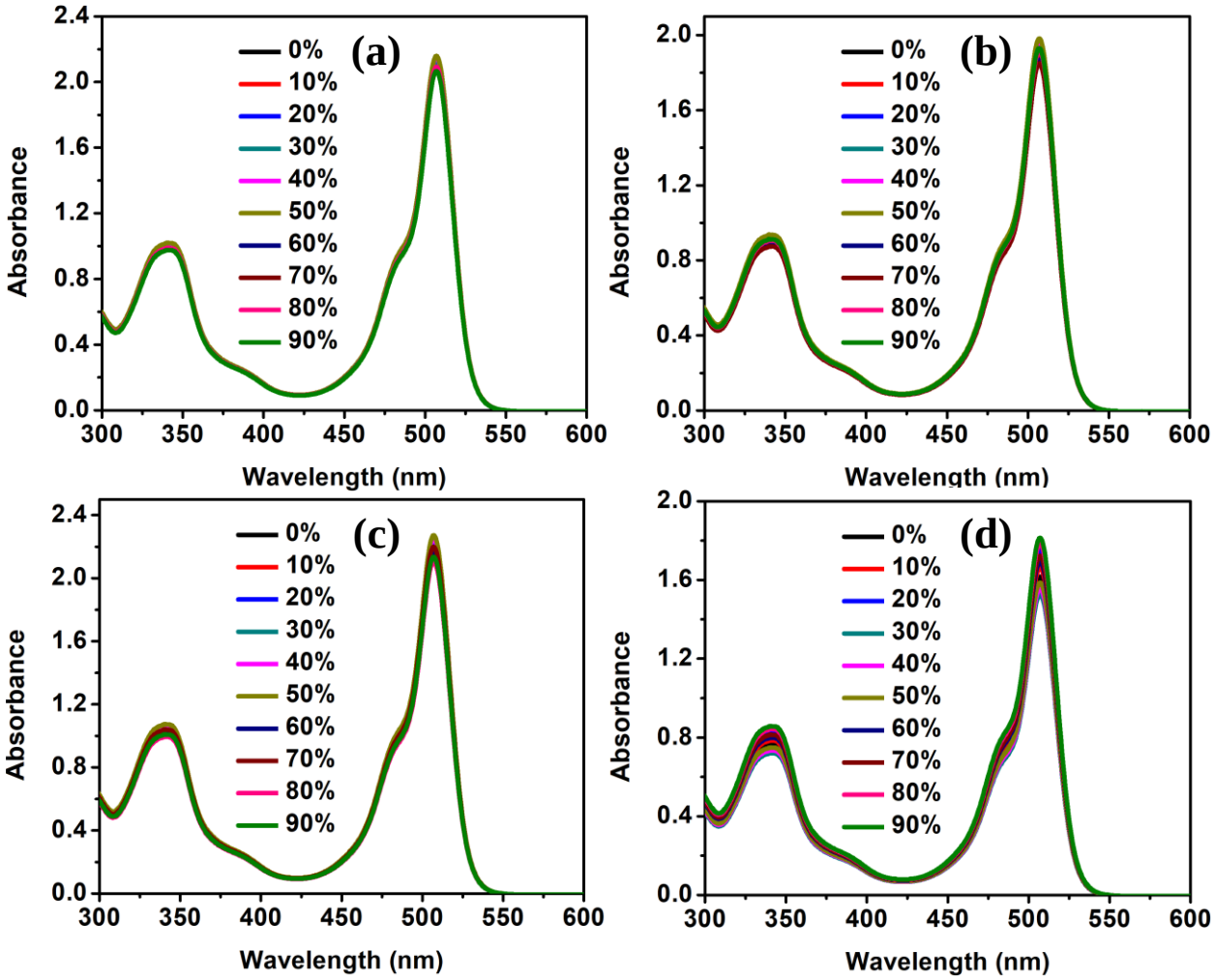

Fig. S45 Absorption spectra of **HPIB1** (a), **HPIB2** (b), **HPIB3** (c) and **HPIB4** (d) in methanol/glycerol mixture with varying glycerol volume fractions (c; 50 μM).

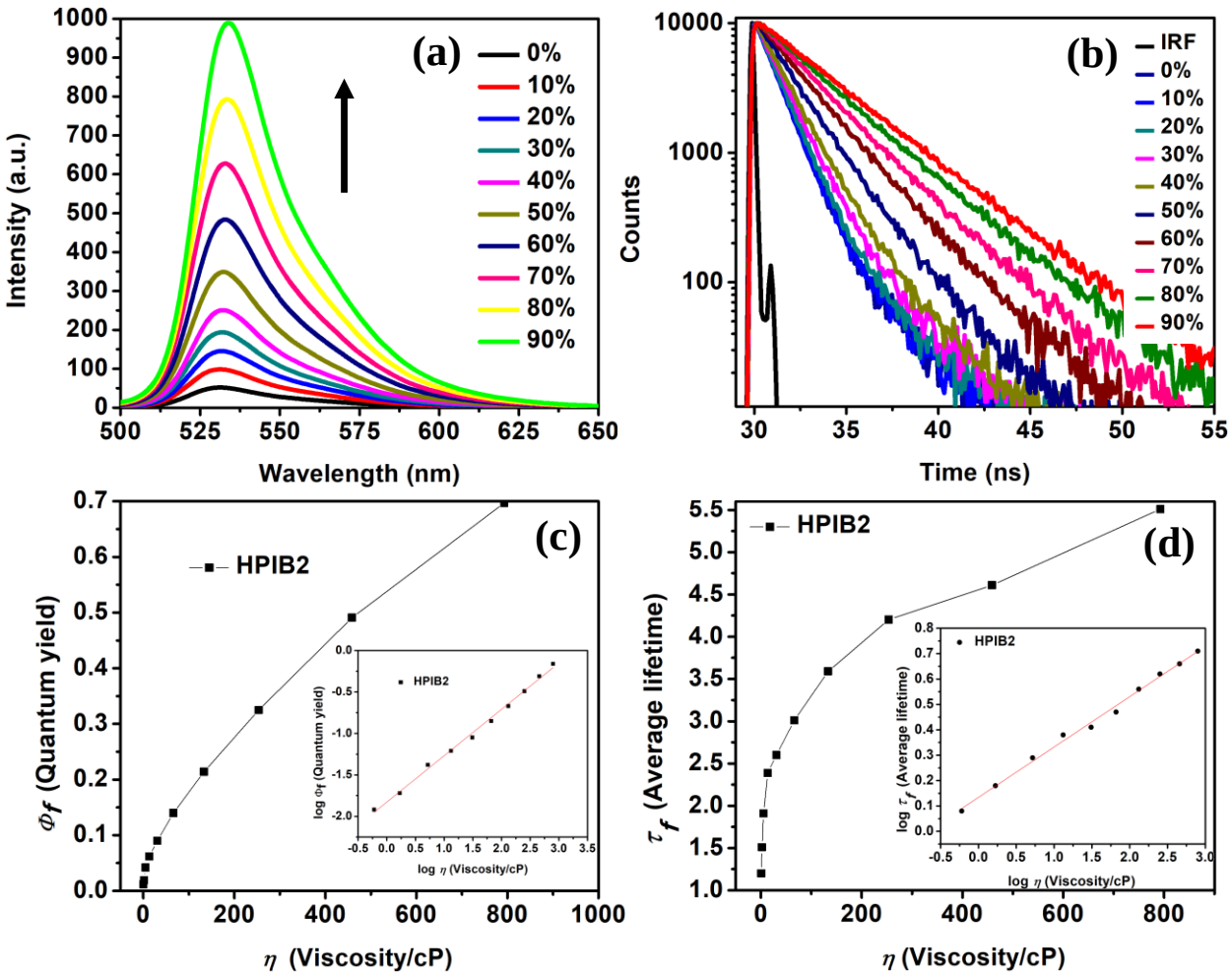

Fig. S46 (a) Emission spectra (c; 50 μM, DMF, λ_{ex}; 505 nm) and, (b) time-resolved fluorescence decay profile (λ_{ex} = 482 nm and λ_{em} = ~535 nm), at different viscosities of medium (in methanol/glycerol mixtures) (c) plot of fluorescence quantum yield (Φ_f) as a function of viscosity; the inset shows the linearity in the entire range of viscosity under investigation obtained in the log plot, (d) plot of fluorescence lifetime (τ_f) as a function of viscosity; the inset shows the linearity in the entire range of viscosity under investigation obtained in the log plot according to the Förster–Hoffmann equation for **HPIB2**.

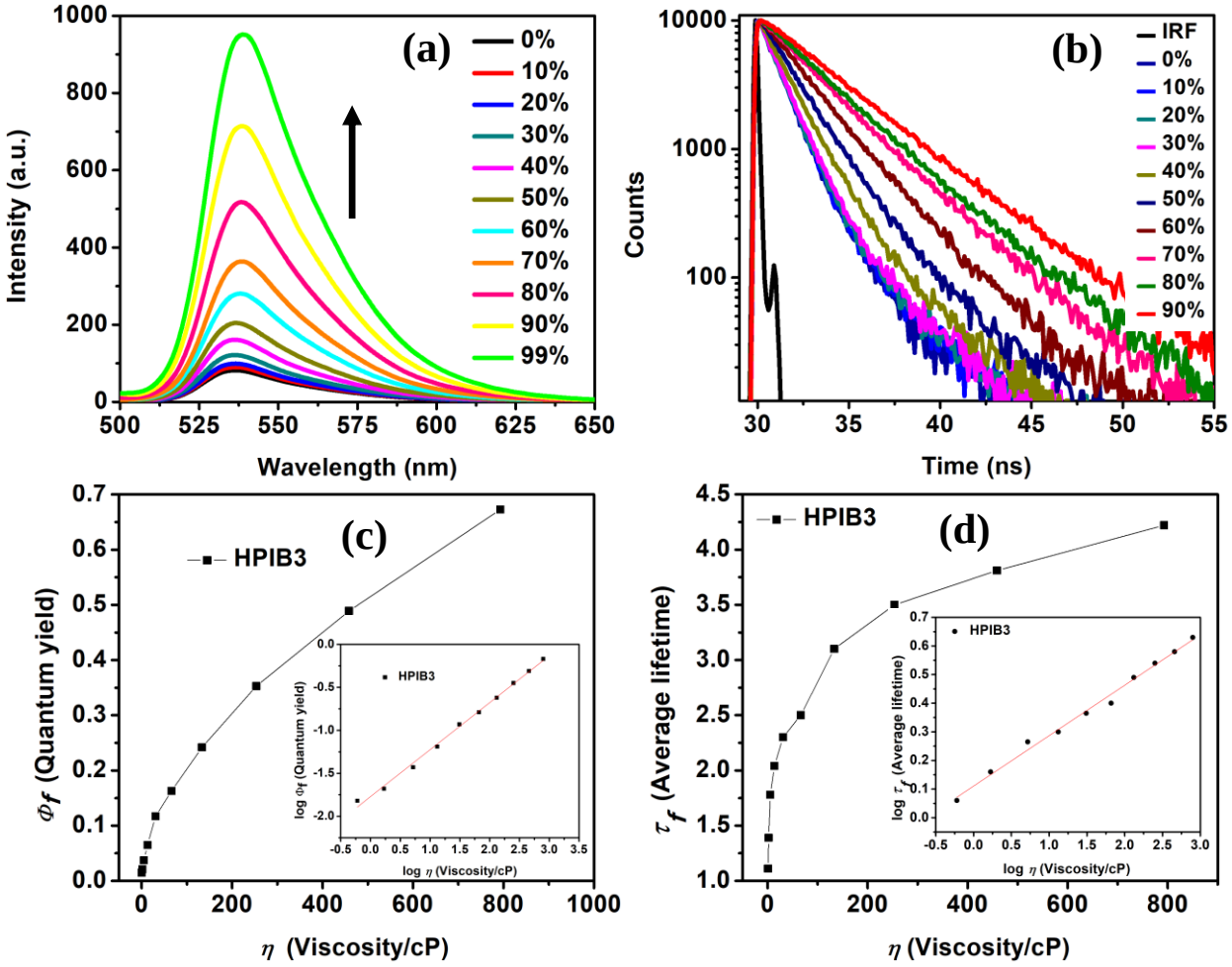

Fig. S47 (a) Emission spectra (c; 50 μM, DMF, λ_{ex}; 505 nm) and, (b) time-resolved fluorescence decay profile (λ_{ex} = 482 nm and λ_{em} = ~535 nm), at different viscosities of medium (in methanol/glycerol mixtures) (c) plot of fluorescence quantum yield (Φ_f) as a function of viscosity; the inset shows the linearity in the entire range of viscosity under investigation obtained in the log plot, (d) plot of fluorescence lifetime (τ_f) as a function of viscosity; the inset shows the linearity in the entire range of viscosity under investigation obtained in the log plot according to the Förster–Hoffmann equation for **HPIB3**.

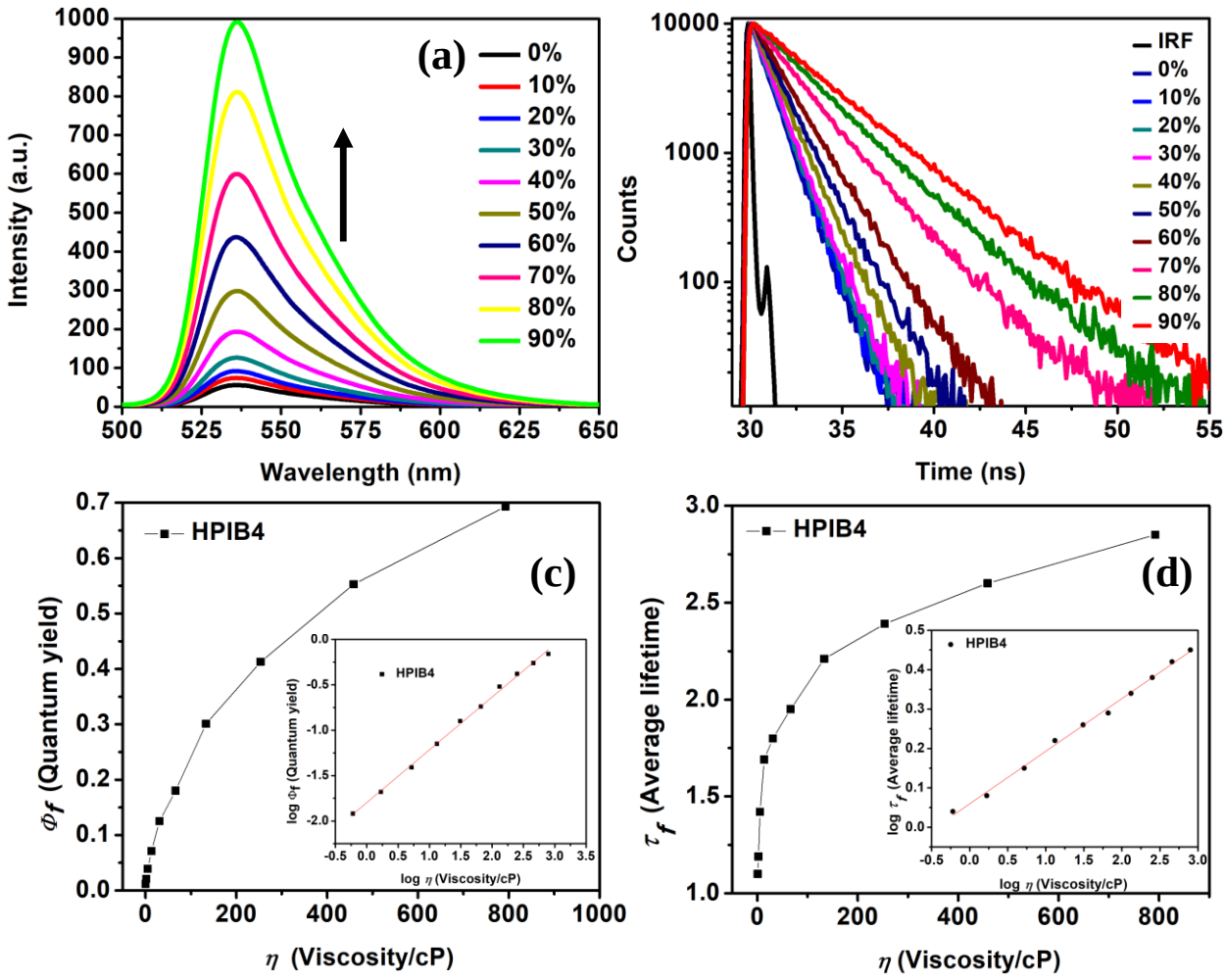

Fig. S48 (a) Emission spectra (c; 50 μM, DMF, λ_{ex}; 505 nm) and, (b) time-resolved fluorescence decay profile (λ_{ex} = 482 nm and λ_{em} = ~535 nm), at different viscosities of medium (in methanol/glycerol mixtures) (c) plot of fluorescence quantum yield (Φ_f) as a function of viscosity; the inset shows the linearity in the entire range of viscosity under investigation obtained in the log plot, (d) plot of fluorescence lifetime (τ_f) as a function of viscosity; the inset shows the linearity in the entire range of viscosity under investigation obtained in the log plot according to the Förster–Hoffmann equation for **HPIB4**.

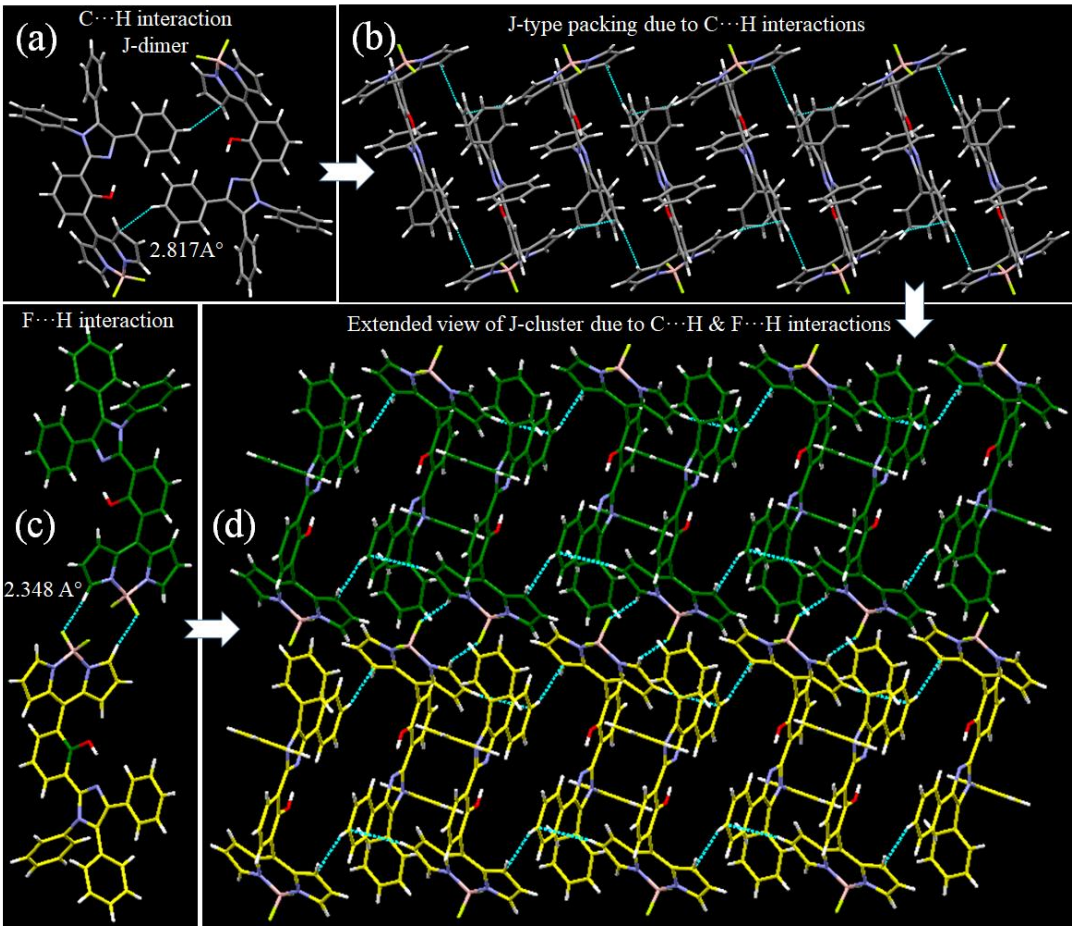

Fig. S49 (a) J-dimer structure due to C–H···π interactions. (b) J-aggregates due to C–H···π interactions. (c) Dimer structure due to B–F···H–C interaction. (d) Extended view of the J-clusters due to C–H···π and B–F···H–C type interactions extracted from single crystal XRD data of **HPIB1**.

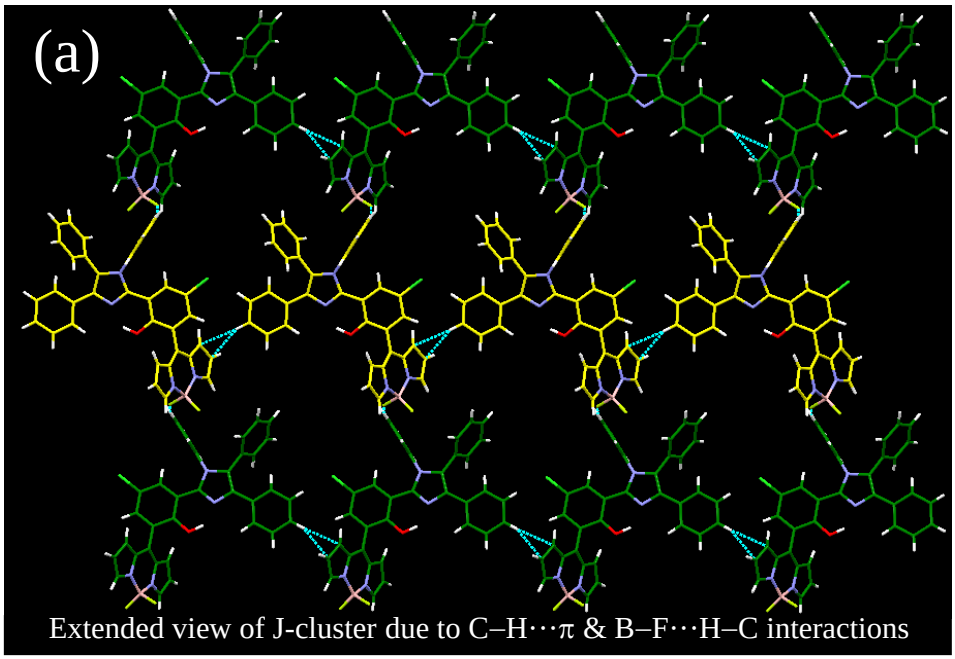

Fig. S50 (a) Extended view of the J-clusters due to C–H···π and B–F···H–C type interactions extracted from single crystal XRD data of **HPIB2**.

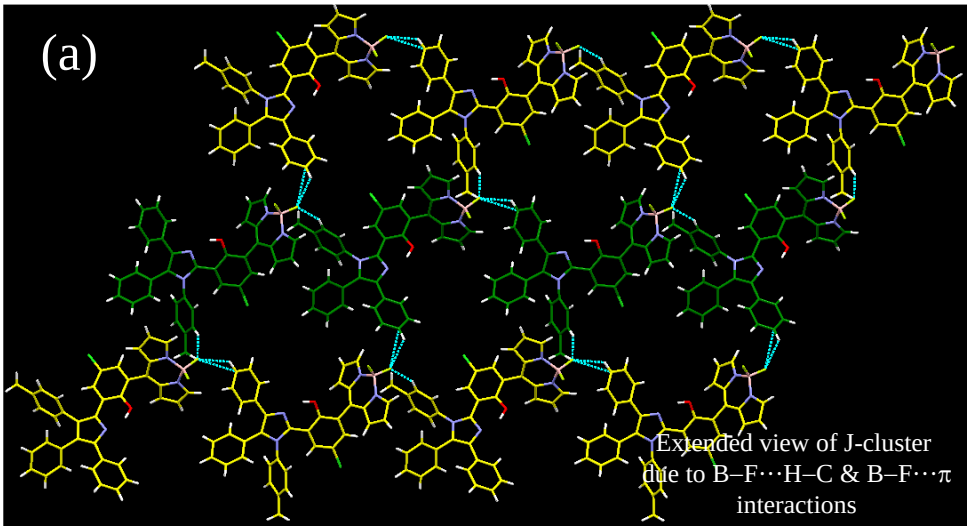

Fig. S51 (a) Extended view of the J-clusters due to B–F···H–C and B–F···π type interactions extracted from single crystal XRD data of **HPIB3**.

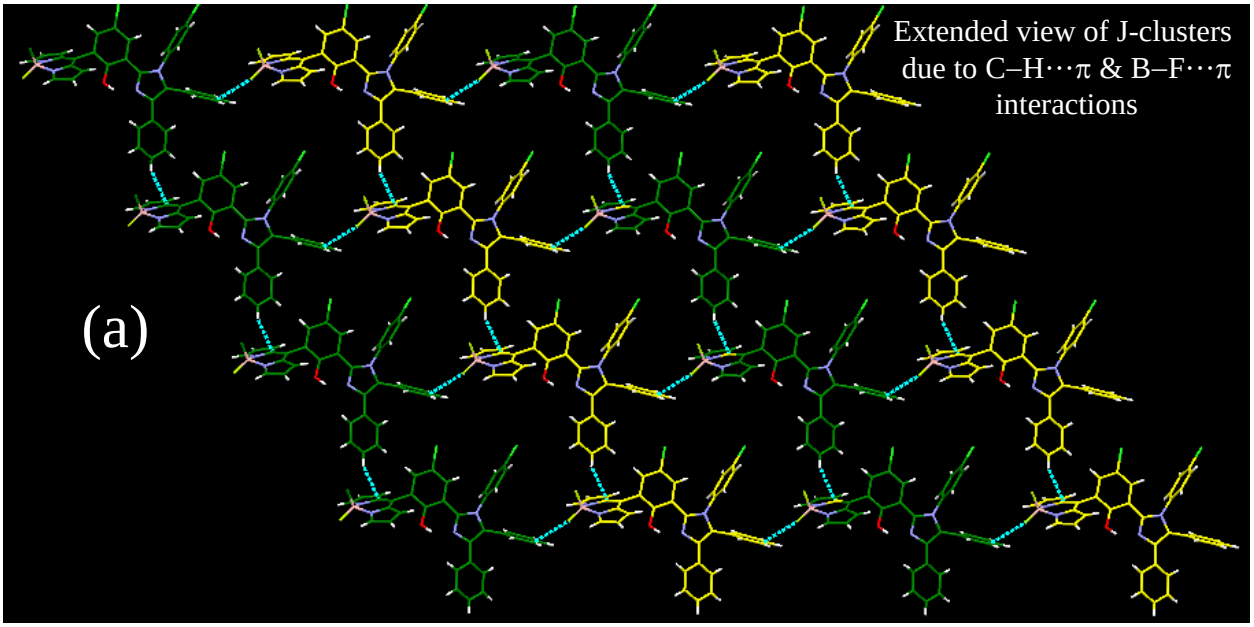

Fig. S52 (a) Extended view of the J-clusters due to C–H···π and B–F···π type interactions extracted from single crystal XRD data of **HPIB4**.

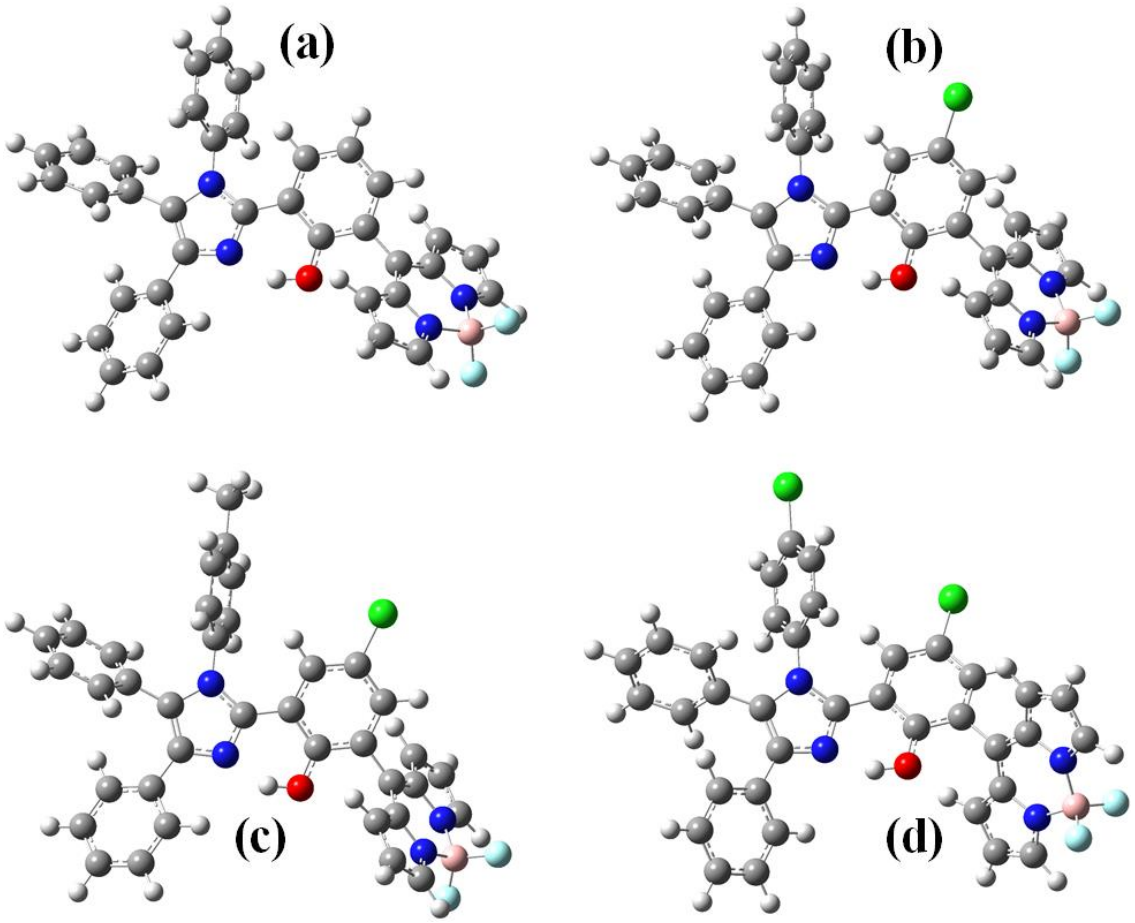

Fig. S53 DFT optimized Structure for **HPIB1** (a), **HPIB2** (b), **HPIB3** (c) and **HPIB4** (d).

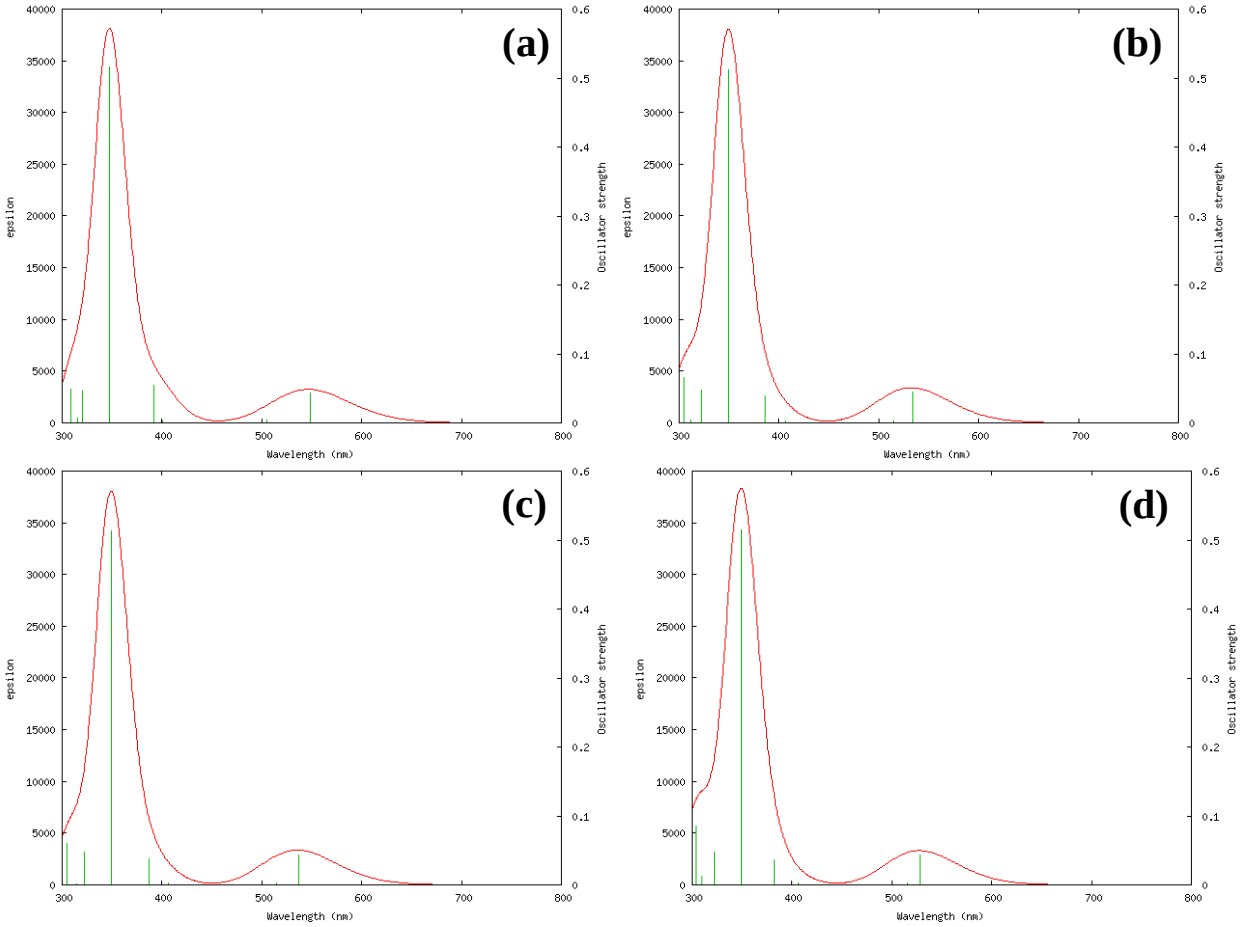

Fig. S54 UV/Vis spectra of **HPIB1** (a), **HPIB2** (b), **HPIB3** (c) and **HPIB4** (d) from TD-DFT calculations.

Table S1 Calculated fluorescence yield (Φ_f) in different solvents for **HPIB1**–**HPIB4**

Solvents	**Fluorescence quantum yields (Φ_f)**			
	HPIB1	**HPIB2**	**HPIB3**	**HPIB4**
Hexane	0.037	0.067	0.007	0.009
Benzene	0.130	0.577	0.578	0.172
Toluene	0.107	0.560	0.579	0.179
Chloroform	0.103	0.371	0.467	0.089
THF	0.072	0.338	0.413	0.071
DCM	0.097	0.370	0.398	0.088
DMSO	0.032	0.047	0.063	0.027
DMF	0.039	0.053	0.059	0.033
MeCN	0.017	0.044	0.019	0.012
MeOH	0.011	0.013	0.016	0.014

[Fluorescence quantum yield (Φ_F) for these compounds (**HPIB1**–**HPIB4**) have been calculated relative to rhodamine 6G dye (H_2O, λ_{ex} = 530 nm, λ_{em} = 552 nm, Φ = 0.95) as a reference using the formula [$(\Phi_F = \Phi_R \times (I_T/I_R) \times (A_R/A_T) \times (\eta_T^2/\eta_R^2)$], where Φ = quantum yield, I = area under the curve of emission spectrum, A = absorbance at λ_{ex}, η = refractive index of solvent. The subscript R and T denote values for the reference and test samples respectively. Stock solutions for **HPIB1**–**HPIB4** have been prepared in DMF.]

Table S2. Fluorescence lifetime (τ_f) variation at different viscosities (in methanol/glycerol mixtures) for **HPIB1**–**HPIB4**

Glycerol volume fractions	**Viscosity (η)/cP**	**Average life-time (τ_f)/ns**			
		HPIB1	**HPIB2**	**HPIB3**	**HPIB4**
0%	0.6	1.10	1.20	1.11	1.10
10%	1.8	1.30	1.51	1.39	1.19
20%	5.2	1.61	1.91	1.78	1.42
30%	13.2	1.79	2.39	2.04	1.69
40%	30.6	2.11	2.60	2.30	1.80
50%	66.0	2.32	3.01	2.50	1.95
60%	133.2	2.73	3.59	3.10	2.21
70%	253.5	3.05	4.21	3.50	2.39
80%	458.6	3.41	4.61	3.81	2.60
90%	793.0	3.62	5.51	4.22	2.85

(Average lifetime is given; ns = nanosecond; excitation wavelength is 482 nm)

Table S3 Fluorescence quantum yield (Φ_f) variation at different viscosities (in methanol/glycerol mixtures) for **HPIB1**–**HPIB4**

Glycerol Volume fractions	**Viscosity (η)/cP**	**Fluorescence quantum yield (Φ_f)**			
		HPIB1	**HPIB2**	**HPIB3**	**HPIB4**
0%	0.6	0.009	0.012	0.015	0.012
10%	1.8	0.021	0.019	0.021	0.021
20%	5.2	0.036	0.042	0.037	0.039
30%	13.2	0.050	0.062	0.065	0.071
40%	30.6	0.08	0.090	0.117	0.125
50%	66.0	0.151	0.140	0.163	0.180
60%	133.2	0.235	0.214	0.242	0.301
70%	253.5	0.349	0.325	0.353	0.413
80%	458.6	0.527	0.491	0.489	0.553
90%	793.0	0.670	0.697	0.673	0.693

[Fluorescence quantum yield (Φ_F) for these compounds (**HPIB1**–**HPIB4**) have been calculated relative to rhodamine 6G dye (H_2O, λ_{ex} = 530 nm, λ_{em} = 552 nm, Φ = 0.95) as a reference using the formula [($\Phi_F = \Phi_R \times (I_T/I_R) \times (A_R/A_T) \times (\eta_T^2/\eta_R^2)$], where Φ = quantum yield, I = area under the curve of emission spectrum, A = absorbance at λ_{ex}, η = refractive index of solvent. The subscript R and T denote values for the reference and test samples respectively. Stock solutions for **HPIB1**–**HPIB4** have been prepared in DMF.]

Table S4 Variation in radiative (kr) and non-radiative (knr) rate constants in methanol/glycerol mixture at different viscosities for **HPIB1**–**HPIB4**

Glycerol Volume fractions	**Viscosity (η)/cP**	**HPIB1**		**HPIB2**		**HPIB3**		**HPIB4**	
		Kr	***Knr***	***Kr***	***Knr***	***Kr***	***Knr***	***Kr***	***Knr***
0%	0.6	0.0081	0.90	0.010	0.82	0.013	0.89	0.011	0.90
10%	1.8	0.0161	0.75	0.012	0.65	0.015	0.70	0.018	0.82
20%	5.2	0.0225	0.60	0.022	0.60	0.021	0.54	0.027	0.68
30%	13.2	0.0280	0.53	0.026	0.52	0.032	0.46	0.042	0.58
40%	30.6	0.038	0.44	0.035	0.43	0.051	0.38	0.069	0.49
50%	66.0	0.0650	0.37	0.046	0.28	0.065	0.33	0.092	0.42
60%	133.2	0.086	0.28	0.060	0.22	0.078	0.24	0.014	0.32
70%	253.5	0.114	0.21	0.077	0.17	0.100	0.18	0.170	0.25
80%	458.6	0.154	0.14	0.110	0.11	0.130	0.13	0.210	0.17
90%	793.0	0.185	0.09	0.130	0.054	0.160	0.077	0.240	0.11

(kr and knr are calculated using the formula, $kr = \Phi_f/\tau_f$ and $knr = (1-\Phi_f)/\tau_f$)

Table S5 Selected bond distances extracted from the crystal structure of **HPIB1−HPIB4** and their comparison with DFT optimized structure

Bond length (Å)	**HPIB1**		**HPIB2**		**HPIB3**		**HPIB4**	
	Crystal	DFT optimized	Crystal	DFT optimized	Crystal	DFT optimized	Crystal	DFT optimized
N1–B1	1.534(7)	1.567	1.539(4)	1.568	1.548(3)	1.568	1.557(3)	1.568
N2–B1	1.525(7)	1.567	1.533(4)	1.568	1.547(3)	1.568	1.544(3)	1.568
B1–F1	1.350(7)	1.382	1.416(5)	1.381	1.382(2)	1.382	1.358(3)	1.381
B1–F2	1.407(7)	1.385	1.416(5)	1.384	1.376(2)	1.384	1.387(3)	1.384
C5–C10	1.392(6)	1.489	1.492(3)	1.490	1.493(2)	1.490	1.493(2)	1.490
O1–C11	1.355(5)	1.339	1.342(3)	1.338	1.3441(19)	1.337	1.339(2)	1.338
C12–C16	1.475(6)	1.469	1.467(4)	1.469	1.468(2)	1.469	1.468(3)	1.469
C16–N3	1.321(5)	1.329	1.324(3)	1.328	1.328(2)	1.329	1.323(2)	1.328
C17–C18	1.376(5)	1.385	1.372(4)	1.386	1.376(2)	1.386	1.367(3)	1.385
C17–C19	1.465(6)	1.474	1.472(4)	1.474	1.474(2)	1.474	1.367(3)	1.474
C18–C25	1.469(6)	1.477	1.484(3)	1.477	1.474(2)	1.477	1.477(3)	1.477
C18–N4	1.405(5)	1.403	1.390(3)	1.402	1.398(2)	1.402	1.395(2)	1.404
C16–N4	1.371(5)	1.382	1.373(3)	1.381	1.3740(19)	1.380	1.373(2)	1.382
N4–C31	1.449(5)	1.436	1.445(3)	1.436	1.442(2)	1.436	1.441(2)	1.434

Table S6 Selected bond angles extracted from the crystal structure of **HPIB1−HPIB4** and comparison with DFT optimized structure

Bond Angle (°)	**HPIB1**		**HPIB2**		**HPIB3**		**HPIB4**	
	Crystal	**DFT**	**Crystal**	**DFT**	**Crystal**	**DFT**	**Crystal**	**DFT**
F1–B1–F2	108.8(5)	111.47	108.9(3)	111.53	109.76(16)	111.51	110.61(18)	111.53
N2–B1–N1	107.4(4)	104.89	106.4(2)	104.89	105.40(14)	104.91	104.75(16)	104.92
C4–C5–C10	121.4(4)	121.03	120.2(2)	120.95	119.85(15)	120.88	120.29(17)	120.78
C10–C5–C6	118.3(4)	119.03	119.5(2)	118.94	119.60(14)	119.01	119.09(17)	119.05
C11–C10–C5	119.0(4)	119.03	120.8(2)	121.06	120.15(14)	120.91	120.49(16)	120.85
C15–C10–C5	121.5(4)	121.04	119.1(2)	118.89	119.83(14)	118.99	119.20(16)	119.06
O1–C11–C10	115.3(4)	117.69	117.7(2)	117.76	117.81(14)	117.72	116.95(16)	117.74
C16–N3–C17	108.5(3)	108.31	108.1(2)	108.26	107.57(14)	108.27	108.01(15)	108.32
N3–C17–C19	118.7(4)	120.42	120.6(2)	120.47	120.27(14)	120.49	120.11(16)	120.48
C17–C18–C25	131.3(4)	131.22	131.5(2)	131.18	131.08(16)	131.13	130.66(18)	131.17
C18–N4–C16	107.6(3)	107.41	107.5(2)	107.37	107.44(13)	107.38	107.21(15)	107.37
C16–N4–C31	129.0(4)	128.20	129.2(2)	128.17	128.92(13)	128.19	128.82(16)	128.27

Table S7 Dihedral angles extracted from the crystal structure of **HPIB1−HPIB4** and comparison with DFT optimized structure

	HPIB1		**HPIB2**		**HPIB3**		**HPIB4**	
	Crystal	**DFT**	**Crystal**	**DFT**	**Crystal**	**DFT**	**Crystal**	**DFT**
Between **BODIPY core** and phenyl ring **A**	80.93°	66.95°	61.85°	66.16°	60.68°	66.45°	71.22°	66.95°
Between **imidazole ring** and phenyl ring **A**	3.08°	15.40°	6.34°	15.70°	12.86°	14.78°	3.13°	15.40°
Between **imidazole ring** and phenyl ring **B**	86.68°	71.56°	83.83°	73.53°	73.94°	73.67°	87.05°	71.56°
Between **imidazole ring** and phenyl ring **C**	76.34°	58.15°	72.21°	58.35°	50.57°	58.04°	78.27°	58.15°
Between **imidazole ring** and phenyl ring **D**	3.39°	28.86	3.34°	28.90°	32.16°	28.99°	23.21°	28.86°

Table S8 Electronic transitions obtained through TD-DFT calculation for **HPIB1**−**HPIB4**

Compounds	E/ev	E/nm	Oscillator strength	Contributions
HPIB1	2.26	548.53	0.0431	H->L (98%), H-4->L (2%)
	3.16	391.74	0.0541	H-4->L (90%), H-3->L (5%), H->L (2%)
	3.57	347.76	0.5159	H-3->L (70%), H-2->L (18%), H-11->L (6%), H-4->L (6%)
	3.87	320.15	0.0455	H-8->L (29%), H-7->L (69%)
HPIB2	2.32	533.56	0.0443	H->L (97%), H-4->L (2%)
	3.21	385.76	0.0388	H-4->L (93%), H-3->L (3%), H->L (2%)
	3.56	349.64	0.5123	H-3->L (77%), H-2->L (13%) H-11->L (7%), H-4->L (3%)
	3.84	322.68	0.0474	H-7->L (98%)
HPIB3	2.31	536.89	0.0439	H->L (97%), H-4->L (2%)
	3.21	387.02	0.0382	H-4->L (93%), H-3->L (3%), H->L (2%)
	3.55	349.49	0.5127	H-3->L (77%), H-2->L (13%) H-11->L (7%), H-4->L (3%)
	3.84	322.64	0.0472	H-7->L (95%), H-8->L (3%)
HPIB4	2.35	528.42	0.0432	H->L (97%), H-4->L (2%)
	3.24	382.45	0.0368	H-4->L (93%), H-3->L (2%), H->L (2%)
	3.55	349.36	0.5149	H-3->L (78%), H-2->L (13%) H-11->L (6%), H-4->L (3%)
	3.84	322.629	0.0478	H-7->LUMO (99%)